Tectonosedimentary evidence in the Tunisian Atlas, Bou Arada Trough: insights for the geodynamic evolution and Africa-Eurasia plate convergence

Mohamed Ben Chelbi, Kamel Samir, Harrab Salah, Rebai Noemen, Melki Fetheddine, Mustapha Meghraoui, Zargouni Fouad

Tectono-sedimentary evidence in the Tunisian Atlas - Bou Arada Trough: Insights for the geodynamic evolution and Africa-Eurasia plate convergence

Mohamed Ben Chelbi[1 2*], Samir Kamel[1], Salah Harrab[1],
Noemen Rebaï[3], Fetheddine Melki[1], Mustapha Meghraoui [4], Fouad Zargouni[1]

[1] Laboratoire de Géologie Structurale et Appliquée, Faculté des Sciences de Tunis, Université Tunis El Manar 2092, Tunis, Tunisie
[2] Institut Supérieur des Sciences et Techniques des Eaux de Gabès, Université de Gabès, Cité Erriadh, 6072 Zrig Gabès, Tunisie
[3] Unité Bassin Sédimentaire, Université Tunis El Manar, 1092, Tunis, Tunisie.
[4] EOST Institut Physique de Globe, Université de Strasbourg, France

***Corresponding author: (med.benchelbi@gmail.com)**

Abstract:

The Bou Arada Trough (BAT) is an E-W oriented structure located 80 km SW of Tunis, characterizing the central Tunisian Atlas. This trough is filled by a thick Quaternary sand and clay series and is bordered by complex systems of folds generally trending NE-SW. Contacts between the BAT and the neighbouring folds are accommodated by NE-SW and NW-SE oriented faults. Contrary to the other troughs of the Tunisian Atlas, which are related to the Plio-Quaternary orogenic period, the geodynamic evolution of the BAT has been started since began in the Maastrichtian and has continued until the present day. Structural, tectono-sedimentary and seismic data analyses are undertaken in the studied area to better understand the evolutionary scenario of this trough. Results obtained show that the BAT is fragmented into three NW-SE oriented sub-basins and records a continuous history of downthrow. Indeed, during extensional to transtensional regimes, this trough has evolved in response to the two networks of perpendicular fractures while during compressive to transpresssive periods, the collapse of the BAT has been induced by a pull-apart mechanism using the same

network of faults but with a strike slip movement. The Bou Arada Trough thus preserves a record of the convergence between the European and African plates since the Maastrichtian.

Key Words:

Bou Arada Trough, Geodynamic evolution, Tunisian Atlas, Transtension, Rifting, Transpression, pull-apart basin, Eurasia-Africa convergence.

1. Introduction

The present configuration of the Tunisian margin has resulted from the convergence and collisional movement between the African and European plates including the Tethys geological domain. The central Tunisian Atlas and the Algerian Sahara Atlas mountain ranges contain several troughs filled with Quaternary deposits arranged in a structural band between the Zaghouan and Teboursouk master faults (Fig. 1A). The average trend of these grabens is NW-SE to WNW-ESE, orthogonal to a set of NE-SW trending folds (Fig. 1B). Castany (1948) and Glangeaud (1951) deduced that these structures developed during Plio-Quaternary orogenic phases. These hypotheses were reinvestigated by Jauzein (1967), Richet (1971), Dlala et al. (1983), Philip et al. (1986) and Chihi and Philip (1998). These authors linked the development of these troughs to slip on the E-W and NE-SW faults, so that the grabens resulted from a compressive tectonic regime related to the convergence between African and European plates (Bousquet and Philip, 1986; Ricou, 1994). Although Plio-Quaternary tectonic movements are significant, our recent work (Ben Chelbi, 2007; Ben Chelbi et al., 2008), based on structural, tectono-stratigraphic and seismic analyses, shows that the Tunisian troughs have developed since the Maastrichtian.

The ESE-WNW to E-W Bou Arada Trough (BAT), the target of our present study, is located ~ 80km southwest of Tunis (Fig. 1) and, unlike the other Tunisian Atlas troughs, was not studied by our predecessors. The aims of this work are: (1) to analyze the contacts between this trough and the neighbouring structures; (2) to explore the deep geometry of this structure using three seismic lines; (3) to examine the spatial and temporal changes in facies and thickness of the stratigraphic sequences since Campanian time; (4) to define and characterize links between the evolutionary model of the BAT and the rest of the Tunisian margin; and (5) to correlate the evolution of this graben with other examples in neighbouring regions.

2. Methodology

The study of tectonic contacts between the BAT and neighbouring geological structures is primarily inferred from cross sections and analysis of fault movements. Ten geological cross sections show the current dynamics of the different faults bordering the BAT. In addition, we devote a particular care to the various geometries of these bordering faults. Four seismic sections obtained from the Tunisian Petroleum Company (ETAP), are interpreted in this study to illustrate the main structural geometry of the BAT at depth. The W1 petroleum well is used to show the succession of different stratigraphic sequences characterizing the trough using time-depth conversion of lithological data.

The geodynamic evolution of the BAT is interpreted, first, through the analysis of vertical facies variations and thicknesses of the different series on both sides of the NW-SE oriented faults. Since the Campanian, sedimentation has been controlled by this network of faults in which we note a large variation of facies and thicknesses. Second, palaeostress regimes are obtained by measurement of syn-depositional faults. These fault plane orientations and directions and senses of slips are subsequently analyzed using Angelier's (1984, 1989) Direct

Inversion Method (software version 5.42). This combination of surface and sub surface data will contribute to the development of an evolutionary scenario for the BAT.

3. Geological setting

3.1. Stratigraphy

The stratigraphic series outcropping in the study area are essentially of Triassic, Cretaceous and Palaeogene age (Figs 2 and 3). Triassic beds crop out in Jebel Ech Chehid and Jebel Bessioud (Fig. 3B), composed of clay, marl, limestone, gypsum, salt, anhydrite and sand. The Germanic facies of Triassic, typical of the Tunisian margin, is evident. The Early Cretaceous is formed by thick series of clay, limestone and rare quartzitic intercalations. This sedimentation characterizes the “Sillon tunisien” (Sekatni et al, 2008). The Late Cretaceous is represented by carbonate and argillaceous sedimentation. It begins with alternations of gray marl and limestone (Fig. 3). These alternations characterize the Fahdène and Bahloul Formations, respectively of Albian and Cenomano-Turonian ages (Burollet, 1956). The middle part of the Late Cretaceous corresponds to the argillaceous Aleg Formation, allotted to the Turonian-Coniacian-Santonian-Middle Campanian (Burollet, 1956). The Abiod Formation, Late Campanian to Maastrichtian in age, is composed of two limestone beds inter-bedded by marl (Fig. 3). The Tertiary is represented by Palaeocene clay (El Haria Formation), Early Eocene limestone (Bou Dabbous Formation), Late Eocene clay (Souar Formation) and Oligocene alternations of sand and clay (Fortuna Formation). These Tertiary sequences mark marine sedimentation during the Palaeocene and Eocene, and continental units of the Oligocene period. These various Palaeogene units are unconformably covered by Mio-Pliocene continental deposits formed essentially of sands and silt (Fig. 3).

3.2. Structural evolution

The geodynamic evolution of the Tunisian Atlas Mountains and margin has been part of the Tethys geological domain from the first stages of rifting until the present stage of the collision between Eurasia and Africa (Fig. 4). Evidence of first stages of the Tethyan rifting are dated to the Jurassic (Alouani et al., 1992; Soussi and Ben Ismaïl, 2000; Soussi, 2003; Boughdiri et al., 2006; Sekatni et al., 2008; Fig. 4). This Jurassic rifting phase has been inferred from the alkaline composition of the igneous rocks and in the presence of radiolarians in rocks associated with the middle Jurassic series. This rifting resulted from N-S extension and this mechanism of opening continued during the Early Cretaceous (Letouzey and Trémolière, 1980; Soyer and Tricart, 1987; Morgan et al., 1998). The minimum stress direction was NE-SW until the Aptian (Soyer and Tricart, 1987; Ben Chelbi et al., 2008; Melki et al., 2010; Fig. 4). This change in the minimum stress orientation was attested by reactivation of the NW-SE trending faults with normal activity, which created several basins elongated NE-SW (Ben Chelbi et al., 2008), and by intense magmatic activity associated with sedimentation. Contemporaneous to this activity, the Tunisian Atlas records intense halokinetic activity (Fig. 4) forming a large system of diapirs and/or salt glaciers (Vila et al. 1994).

During Late Cretaceous the Tunisian margin was controlled by transtensional tectonics (Zouari et al., 1999; Ben Chelbi et al. 2008), characterized by reactivation of the N-S, E-W and NE-SW trending normal faults with dextral component. The general inversion of the structures was recorded during the Middle Eocene (Masrouhi et al., 2008; Melki et al., 2010). The first period of folding is assigned to the Tortonian (Tlig et al., 1991), while the ultimate compression leading to the building of the Tunisian Atlas Mountains began during the Villafranchian and continues to the present-day (Bouaziz et al., 2002; Fig. 2). This long period of compression controlled by NNW-SSE to N-S stress has contributed to the final configuration of the Tunisian Atlas in which NE-SW, NW-SE, E-W and N-S oriented faults were respectively reactivated with sinistral reverse, dextral reverse, reverse and sinistral slip**.**

The central Tunisian Atlas is characterized by the coexistence of folding and rifting (Fig. 1B). The anticlines and large syncline basins that developed in this part of the Tunisian Atlas and are generally filled up with by Late Eocene deposits are elongated NE–SW. NW-SE oriented rifts, filled up by Mio-Plio-Quaternary deposits, developed orthogonally to these folds (Philip et al., 1986). The NE-SW oriented sinistral and NW-SE oriented dextral normal faults ensured the formation of these rifts following a pull-apart model (Ben Ayed and Viguier, 1981).

Evaporite layers, mostly Triassic in age, are present as a deep decollement level (Ahmadi et al. 2006). During both extensional and compressional phases this Triassic salt has been remobilized throughout the preexistent system of faults. Some of them are considered as diapirs (Gharbi et al. 2005) in which salt occupies the core of the anticlines, others as salt glaciers (Ben Chelbi et al. 2006; Ben Slama et al. 2009) in which Triassic evaporites were interstratified within the Aptian clay series. These salt structures started to grow during the Aptian (Snoke et al., 1988; Perthuisot et al., 1998) or even earlier (Boukadi and Bedir, 1996).

These different tectonic phases that affected the Tunisian margin since the first stage of rifting have affected the structural zoning of Tunisia. The major domains are, respectively, from north to south: the Tell zone; the Atlasic domain, itself subdivided into the northern, central and southern Atlas; the stable Sahara Platform; the Eastern Platform; and the North-South Axis (Fig. 1B).

4. Field studies of the structural position of the BAT

Detailed structural analysis of Quaternary deposits that cover the plain and neighbouring folded structures reveals that the history of the BAT is intimately associated with the activity and the evolution of a complex fault system. We present here the main structural features that border the BAT depression.

158 **4.1. Northern contacts:** The BAT is bounded to the north by Jebel Rihane, Henchire Bou
159 Ftis and Jebel Bessioud (Fig. 2A and B). The contact between these structures and the plain is
160 represented by a complex system of faults having two major NW-SE and NE-SW orientations
161 (Fig. 2B). Indeed, Jebel Sidi Brahim and Aïn Agueb, which consist of Aptian-Albian
162 limestone series, are bordered to the south by NW-SE oriented faults (Fig. 5A).
163 These contacts include the so-called Bou Jlida fault (Fig. 2B) that separates the southern El
164 Aroussa plain and northern Jebel Rihane. Detailed examination of these generally SW dipping
165 faults reveals three generations of striations, oriented S60°E and with weak pitch to the SE
166 and strong pitch to the NW, indicating three phases of tectonic activity. Near Sidi Dakhli, the
167 contact between Late Eocene claystone and Cenomanian limestone is represented by a NE-
168 SW trending normal fault (Fig. 5B). The latter has a fault plane dipping SE with two
169 generations of striations. The first generation has a pitch towards the SW indicating a dextral
170 movement, while the second one has a pitch towards the NE indicating a sinistral sliding
171 movement. The southern side of the Henchir Bou Ftis structure is truncated by several NW-
172 SE trending en echelon faults (Fig. 2B and 5C). All these faults indicate polyphase activity of
173 normal dextral slip with three generations of striations (pitches of 15° to the NW, 45° to the
174 NW and 75° to the SE). In the south-eastern part of the Jebel Bessioud syncline, the
175 Oligocene is missing. Slip on several NW-SE oriented faults has resulted in the submergence
176 of this area below Quaternary alluvial deposits (Fig. 5C). In the east, a NW-SE system of
177 faults delimits the Sabkhet El Korzia depression.
178
179 **4.2. Western Contacts:** The BAT is bordered to the west by the large Triassic diapir of Jebel
180 Ech Chehid (Fig. 2B), which is moulded onto the NE-SW oriented El Alia-Téboursouk fault
181 (Perthuisot and Jauzein, 1974; Ben Slama et al. 2009). The Campanian limestone layers and
182 related geometry of Draa Sidi Haj Amor shows the sinistral movement of this NE-SW fault

(Fig. 2B). This structure constitutes a drag fold formed on the fault which gave rise to the Jebel Ech Chehid diapir. Moreover, at Faïd Ez Zitoun, slip on a SE dipping and NE-SW trending normal fault may explain the subsidence of the El Aroussa plain (Fig. 5D). On the fault plain we measured two generation of striations. The first shows a strong pitch to the SW (60° SW) while the second one has a weak pitch to the SW (20° SW), indicating two phases of tectonic activity.

4.3. Southern Contacts: The contact between the folded structures of Jebel er Remil and Taref Ech Chena, in the south, and the Quaternary plains of El Aroussa, Bou Arada and Sabkhet Taref Ech Chena, in the north, is represented by two NW-SE and NE-SW trending fault systems (Fig. 2B). Indeed, the Mio-Pliocene sand and clay formations covering the Jebel er Remil syncline are truncated by a succession of NW-SE trending normal faults (Fig. 6E). The slickensides on these faults indicate normal slip with a component of dextral slip. The curvature of Jebel Strassif is truncated by a NE dipping and NW-SE trending normal fault (Fig. 6F). A cross section at this location shows that the last movement recorded on this fault is reverse, given the overlap of the Palaeocene Sidi Ali Ben Ali Formation over Oligocene deposits (Fig. 6G) but without the normal faulting movement recorded during periods of extension. The Campanian dome of Aïn Bou Slama is bordered by a NE-SW oriented normal fault involving the downthrown of the Late Eocene Formation of Jebel er Remil (Fig. 6H). The northern periclinal termination of the Cretaceous Jebel Taref Ech Chena anticline is truncated by a network of NW-SE and NE-SW oriented faults (Fig. 6Í) with several generations of striations. On both sides of these faults no variation of thicknesses or facies is observed in the Late Cretaceous (pre-Maastrichtian) series. Further east, the downthrown of the northern part of the Taref Ech Chena structure (Fig. 6J) is accommodated by NW-SE oriented faults (Fig. 2B).

5 Seismic data analysis and graben formation

We have used four seismic profiles P1, P2, P3 and P4, respectively oriented NS, NNE-SSW, E-W and NW-SE across the BAT (Fig. 2B). These seismic profiles are calibrated by the **W1** well.

Profile P1 (Fig. 7) shows that the BAT is bordered on the northern and southern areas by two major faults, named F1 and F2, respectively. At Jebel Rihane, fault F1 shows the downthrow of the Late Campanian calcareous series. The cumulative vertical displacement of this limestone layer is estimated as 1700m. At the surface, F1 corresponds to the Sidi Dakhli fault which places the Late Eocene Formation in contact with the Cenomanian marly-limestone (Fig. 5B). In the south, the BAT is separated from the folded structures by north dipping fault F2. According to vertical displacement between the limestone bed of the Abiod Formation in the centre of the trough and its equivalent forming the Aïn Bou Slama dome, the downthrow is estimated to 1300m. In the same locality, the thick clay series of the Souar Formation is in direct contact with Campanian limestone deposits (Fig. 6H). The general configuration represented by this seismic section is of a negative flower structure in which the maximum subsidence is recorded at the centre of the basin.

Profile P2, with a NNE-SSW orientation, is located west of profile P1 and crosses the principal depocentre of the El Aroussa Trough (Fig. 2B). This profile shows that this trough is formed by two major faults constituting another negative flower structure (Fig 7). The cumulative vertical displacement affecting the top of the Campanian limestone series cropping out at Jebel Zemala and in the centre of the trough is estimated as 2000m. At the surface, the northern fault corresponds to the Jebel Sidi Brahim fault whereas the southern fault corresponds to the Jebel Zemala fault (Figs 2B and 5A).

Profile P3 (Fig. 8) crosses Sabkha Taref Ech Chena and continues through the Triassic diapir of Jebel Ech Chehid (Fig. 2B). It shows that the plain of Bou Arada is compartmentalized, from east to west, into three distinct basins along three NE-SW oriented faults, marked at depth by offset in Triassic units, structure this compartmentalization. These bordering faults of hidden basins have normal slip and show small reverse bends which could be induced by progressive structural inversions.

Profile P4 (Fig. 8) crosses the Bled et Tlili anticline and continues to Jebel Hzem Lessoued (Fig. 2B). It shows that this area of BAT is affected by a NE-SW trending normal fault which is also responsible for the subsidence of the El Aroussa plain. The cumulative vertical displacement recorded on this fault by the reference bed of the Abiod Formation is estimated as 1500m. The depressions revealed by profiles P3 and P4 were filled by Mio-Pliocene sand and clay deposits that cover unconformably the Oligocene series.

6. Tectono-sedimentary evolution since the Campanian

To determine the structural evolution of the BAT, we measured the orientations of striations on fault planes that affect different formations. Syndepositional fault populations, providing direct dating of tectonic events, have been specially analyzed. We then calculated the orientations of the principal stress axes $\boldsymbol{\sigma}$ 1, $\boldsymbol{\sigma}$ 2 and $\boldsymbol{\sigma}$ 3 and the ratio $\boldsymbol{\Phi}$ of principal stress differences [$\boldsymbol{\Phi} = (\boldsymbol{\sigma}\ 2 - \boldsymbol{\sigma}\ 3)/(\boldsymbol{\sigma}\ 1 - \boldsymbol{\sigma}\ 3)$] using the Angelier Direct Inversion Method software version 5.42 (Angelier, 1984, 1989). Several deformational phases affecting the studied area were thus established (see Table 1; also Ben Chelbi, 2007; Ben Chelbi et al., 2008).

The first phase of deformation thus recognised involved extension towards N64°W-S64°E on the NW-SE oriented normal faults during the Coniacian-Campanian. These NE-SW faults show a dextral normal movement involving the uplift of Triassic series. The maximum downthrow and sediment thickness during this phase developed at Jebel Rihane and Aïn Bou

Slam (Fig. 9A). In addition, the activity recorded by this network of faults delimits a high zone with a thin series of sediments, corresponding to the modern BAT (Fig. 9A). The configuration of the sedimentary floor was thus controlled by a succession of horsts and grabens in which the current site of BAT is the uplifted zone and Jebel Rihan and Aïn Bou Slam correspond to the collapsed areas (Fig. 9A').

In the second phase, the Maastrichtian to the Middle Eocene period was characterized by a transpressive to compressive tectonics with the maximum compressive strain oriented in the direction N41°W-S41°E. This was determined by analysis of syndepositional micro-faults affecting the formations that characterize this period (Fig. 10 A). This tectonic regime reactivated the NE-SW striking faults with reverse slip and the NW-SE to E-W striking faults with dextral normal slip (Fig. 10 B). This structural configuration involved the downthrow of NW-SE to E-W oriented blocks, for example in the BAT (Fig. 9 B and B'). We note the significant thickness (150m) of the limestone series forming the upper member of the Abiod Formation, the argillaceous series of the El Haria Formation and the various limestone layers of the Bou Dabbous Formation. These three formations are missing at Jebel Rihane and much reduced at Jebel Bou Ftis in the north and at Jebel Bou Arada Aïn Bou Slama in the south.

The phase of extension oriented N16°E-S16°W during the Late Eocene-Aquitanian was also deduced by analyzing syndepositional micro-faults (Fig. 11A). At this time the NW-SE to E-W oriented normal faults (Fig. 11 B) accommodated subsidence of BAT and the uplift of its neighbouring areas (Fig. 9). The NE-SW to N-S trending fault system also accommodated normal slip, amplifying the subsidence of the trough (Fig. 11 C and D).

During the Middle Miocene, the micro-faults analysed indicate N25°W-S25°E compression associated with the crustal shortening of the Atlas Mountains (Fig. 12 A). This phase reactivated the NE-SW oriented faults with reverse slip and the NW-SE to WNW-ESE system with normal slip (Fig. 12 B). The structures bounding the BAT were folded, maintaining the

downthrown in the interior of the trough (Fig. 12 C and D). The Late Miocene-Pliocene period was marked by continental sedimentation in an extensional tectonic regime associated with a S61°W-N61°E oriented principal strain (Fig. 13 A and B), once again revealed by analysis of micro-faults. The pre-existing faults were reactivated with normal slip that accommodated subsidence in the BAT (Fig. 13 C and D).

From the Early Quaternary to the present, the Atlas Mountains of Tunisia have been subjected to shortening with N-S compressive strain (Letouzey, 1986; Tlig et al., 1991; Mzali and Zouari, 2006; Ben Chelbi et al., 2008; Melki et al., 2010). In our study area this neotectonic regime has reactivated the NW-SE and E-W oriented faults with reverse slip (Fig. 14A). Moreover, the NE-SW and N-S fault system has also been reactivated and shows sinistral movements (Fig. 14B).

7. Discussion

On the basis of our morphostructural, tectono-sedimentary and seismic analyses and interpretations we infer a complex history of development of the BAT since the Maastrichtian. Moreover, this graben presents a particular geometry different from the other troughs of the central Tunisian Atlas. Indeed, this depressed structure, with an ESE-WNW to NW-SE orientation, is fragmented into three sub-basins, each one oriented NW-SE to WNW-ESE. These sub-basins are, from east to west, the Taref Ech Chena, Bou Arada and El Aroussa basins. They are separated by NE-SW trending sinistral faults and are downthrown essentially by the WNW-ESE to NW-SE oriented normal faults (Figs 8 to 14). The evolution of BAT indicates some differences when compared to the other Plio-Quaternary troughs of the central Tunisian Atlas described by Dlala et al. (1983), Philip et al. (1986) and Chihi and Philip (1998), Haj Sassi et al. (2006) and Belghith et al. (2011). Indeed, an intimate relationship exists since the Campanian between the facies distribution and thicknesses, and

307 movements of the NW-SE oriented faults. The BAT shows Palaeogene units unconformably
308 covered by Mio-Pliocene continental deposits. The facies and thicknesses of these formations
309 are largely controlled by a complex system of faults.
310 In principle, two possible scenarios can account for the development of the BAT. The first is
311 extension or transtension, accommodated, on the NW-SE to WNW-ESE and NE-SW to ENE-
312 WSW oriented normal faults; the occurrence of this process would lead to the classification of
313 the BAT as an extension or rift basin. Second, the BAT might develop as a pull-apart basin in
314 response to strike-slip movement associated with compression or transpression (Fig. 15).
315 Our results suggest the following evolutionary model of the BAT (Fig. 10 to 14)**:**
316 (i) - During the Late Maastrichtian to the Middle Eocene, the compressive to transpressive
317 tectonic mode applied a horizontal N319 principal strain and a N220 intermediate extensive
318 strain (Fig. 11A). These strains activate the NE-SW to ENE-WSW oriented faults in reverse
319 to dextral reverse movement (Fig. 10 B). The NW-SE to WNW-ESE oriented faults are
320 reactivated into normal mechanism with considerable dextral component (Fig. 10 B). The
321 interference of sliding movements recorded on these bordering faults coupled with the normal
322 movement of the sub-parallel faults to the maximum stress, involves the subsidence of BAT
323 (Fig. 10 C) due to a pull-apart mechanism of opening (Fig. 10 D and Fig. 15). This syn-
324 deposits activity is attested by the total absence of the Maastrichtian, Paleocene and Early to
325 Middle Eocene Formations in Jebel Rihane and Bou Ftis. In parallel, at Jebel Taref Ech
326 Chena, Jebel Bou Arada and Drâa Sidi Haj Amor the equivalent deposits are condensed. At
327 these localities the maximum thicknes of these Formations were lower to 40m (Fig 9).
328 This opening model of BAT is comparable to that proposed for the opening of the Permian
329 basin of Hercynian Morocco described by Saïdia et al. (2002).
330 This considered period is contemporary to the significant convergence between Africa and
331 Eurasia plates (Biju Duval et al., 1977; Dercourt et al., 1985; Carminati et al., 1998;

Carminati and Doglioni, 2004) inducing the obduction of the Maghrebian furrow on the Alboran-Kabylia-Calabria block and the beginning of the thrust-and-fold tectonics that form the Maghreb Atlas Mountains (Piqué et al., 1998; Frizon De Lamotte et al., 2009).

(ii) - During the Late Eocene-Oligocene-Aquitanian interval, the study area was subjected to extension-transpression tectonic regime implying minimum N16 horizontal strain and N269 intermediate compression strain (Fig. 11 A). In response to this strain distribution, NE-SW to ENE-WSW oriented faults have normal mechanism, while the NW-SE to WNW-ESE oriented faults show normal mechanism with oblique component (Fig. 11 B)). This faulting activity shown by the two conjugate systems also involves the uplift of neighbouring structures in the BAT (Fig. 11 C). This syn-sedimentary normal faulting activity is attested by the strong accumulation of the Late Eocene clays and the Oligocene-Aquitanian sands and clays within the graben, and their reduction or absence at Jebel Rihane, Bou Ftis, Jebel Bessioud and Taref Ech Chena (Fig. 9).

This mode of extension tectonics and crustal opening is comparable with the evolution of the Upper Rhine graben (Bergerat, 1977; Granet et al., 2000) which is contemporary to the building of the Numidian basins in Tunisia (Talbi et al., 2008). These extension movements are as well coeval to the opening of the Algerian-Provençal basin (Tapponnier, 1977; Belon and Brousse, 1977) and can be considered as a response to the ongoing convergence between Africa and Eurasia (Biju-Duval et al., 1977; Dercourt et al., 1985).

(iii)- The Middle Miocene ultimate compressive phase responsible for the installation of the Tunisian Atlas (Ben Chelbi et al. 2008) was characterised by a N334 horizontal maximum compression strain, a vertical intermediate extension strain and a N241 oriented minimal strain (Fig. 12 A). These forces reactivated the NE-SW and NW-SE oriented faults in sinistral reverse and dextral to dextral normal movement, respectively (Fig. 12 B). The interaction of movements recorded on these faults may likely guide the continuous opening and subsidence

357 movement of BAT (Fig. 12 C and D). This tectonic configuration is attested by the thick
358 accumulation of Late Miocene continental deposits in the trough centre and their absence in
359 the basin borders.
360 During the Middle Miocene, the North African plate subduction under the Southern European
361 margin was blocked (Dercourt et al., 1985), whereas, the Ionian and Adriatic plates continued
362 to subduct (Aubouin, 1986; Carminati et al., 1998; Doglioni et al., 1999; Faccenna et al.,
363 2004; Panza et al., 2007).
364 (iv) - During the Late Miocene-Pliocene period, the tectonic regime was essentially
365 extensive to transtensive implying a N241 minimal strain and N150 **c**ompressive intermediate
366 strain (Fig. 13 A). This couple of strain distribution reactivated the two pre-existing systems
367 of fractures into normal movement with sinistral and dextral sliding component respectively
368 (Fig. 13 B), thus involving the downthrown of the BAT (Fig. 13 C and D). This activity is
369 here also attested by the strong accumulation of the Mio-Pliocene continental deposits in the
370 centre of the trough, and their absence in its borders.
371 This basin formation mode is similar to that described by Hurwitz et al. (2002) to explain the
372 mode of opening of the Sea of Galilee and the scenario of installation of some troughs of the
373 Pelagean Sea (Chihi and Philip, 1998).
374 (v) - Since the Quaternary until Present day, the tectonic regime affecting the Tunisian
375 Atlas and North Africa Mountain ranges is compressive as shown by the N359 horizontal
376 compressive stress (Meghraoui et al., 1986; Rebai et al., 1992; Fig. 14 A). This most recent
377 tectonic regime reactivates the NE-SW to ENE-WSW and NW-SE to WNW-ESE pre-existent
378 faults in reverse movement with sinistral and dextral sliding component respectively (Fig. 14
379 B). This tectonic phase involves normal faulting and final trough installation in its current
380 architecture (Fig. 14 C). The persistence of this compressive activity causes the reverse
381 movements recorded by all the faults without compensation of the normal movements

recorded since the first extensional phases of this basin's evolution. This configuration is attested, especially, on the P1 and P2 seismic sections. This situation will lead to the beginning of closing of this structure. This period is contemporary to the phase of installation of troughs in the central Tunisian Atlas (Philip et al., 1986; Chihi and Philip, 1998).

8. Conclusions

The BAT has developed during a succession of phases of crustal deformation since the Maastrichtian, in association with slip on major faults oriented NE-SW and NW-SE. It is inferred that during extensional phases the BAT has developed as a rift basin whereas during compressive and transcurrent phases it has developed as a pull-apart basin. Seismic data confirm field observations and indicate that the BAT is segmented into three sub-basins with an overall negative flower structure. Its complex history of development reflects the complex deformation of the wider region as a result of changes in the relative motions of the African and Eurasian plates.

During periods of extensional tectonics the basin subsidence is attributed to a simple rifting model, while during the compressive and transcurrent tectonic periods the opening of this graben occurred according to a pull-apart mechanism. This scenario implies a continuous subsidence in the graben. The examination of seismic profiles combined with field observations reveal 1) the NE-SW oriented faults allowed the fragmentation of this trough in three adjacent grabens, and 2) the bordering faults of this depressed structure show flower structures. Furthermore, the sub-surface observations in seismic profiles confirm those performed at the surface and show that the subsidence process is continuous either in extensional period according to a mechanism of the rifting type or in compression movement period according to a pull-apart mechanism of opening.

Our evolution model of the BAT is different from that proposed to explain the modes of graben formation in the central Tunisian Atlas during the Mio-Plio-Quaternary (Philip et al., 1986). The BAT records the complex tectonic evolution in a convergence, subduction and collision system between the African and Eurasian plates outlined here since the Maastrichtian. Moreover, the BAT structural building could be a potential site for oil and water reservoir because formed by thick Cretaceous and Early Eocene limestone series rich in organic matter and a thick Oligocene and Neogene sandy deposits. Detailed geochemical and hydro-geochemical studies, complementary to this structural analysis, are necessary in order to understand the importance of hydrocarbon and hydrological potentialities within the BAT.

Acknowledgements: This work was made possible with the collaboration of ETAP (Tunisian Petroleum Company) and funding from the Ministry of Higher Education. Field observations and modelling benefited from fruitful discussion with Chedly Abbès and Noureddine Boukadi (Professors at the University of Tunis). We are thankful to Rob Westaway and two anonymous reviewers for the critical reading of an earlier version of the manuscript.

References

Ahmadi, R., Mercier, E., Ouali, J., Mansy, J.L., Van Vliet Lanoe, B., Launeau, P. and Rhekhis, F., 2006. The geomorphological hallmarks of hinges migration in fault related folds. A study case in southern Tunisian atlas. J. Struct. Geol., 28, 721-728.

Alouani, R., Raïs, J., Sahiro, G., Tlig, S., 1992. Les structures en décrochement au Jurassique de la Tunisie de Nord : Témoin d'une marge transformante entre Afrique et Europe. *Comptes Rendus Académie Sciences* Paris, 315, II, 717-724.

Anderson, T.H., & Nourse, J.A., 2005. Pull-apart basins at releasing bends of sistral Late Jurassic Mojave-Sonora fault system. Bull. Geol. Soc. Amer., special publication 393-03, 97-122.

Angelier, J., 1984. Tectonic analysis of fault slip data sets. J. Geophys. Res. 89 (B7), 5835–5848.

Angelier, J., 1989. From orientation to magnitudes in paleostress determinations using fault slip data. J. Struct. Geol. 11 (1/2), 37– 50.

Aubouin, J., 1986. Les grands traits de l'évolution des chaînes de montagnes ; Téthys et Pacifique, collision et subduction. *Unive. Nal. Auton, Mexico, Inst. Geologia, Revista,* 5, 239-253.

Belguith, Y., Geoffroy, L., Rigane, A., Gourmelen, C., Ben Dhia, H., 2011. Neogene extensional deformation and related stress regimes in central Tunisia. *Tectonophysics* 509, 198–207

Bellon, H., Brousse, R., 1977. Le magmatisme périméditerranéen occidental. Essai de synthèse. Bull. Soc. Géol. France 7, XIX, 3, 469-480.

Ben Ayed, N., Viguier, C. 1981. Interprétation structural de la Tunisie Atlasique. *Comptes Rendus Académie des Sciences* Paris.292, II, 1445-1448.

Ben Chelbi, M., 2007. Analyse tectonique des structures liées à la faille de Tunis-Ellès. Thèse Doctorat, Université Tunis, 265p.

Ben Chelbi, M., Melki, F., Zargouni, F., 2006. Mode de mise en place des corps salifères de l'Atlas septentrional. Exemple de l'appareil de Bir Afou. *Comptes Rendus Géosciences* Paris, 338, 349-358.

Ben Chelbi, M., Melki, F., Zargouni, F., 2008. Précision sur l'évolution structurale de l'Atlas septentrional de Tunisie depuis le Crétacé (Bassin de Bir M'Cherga). Echos d'une évolution polyphasée de la marge tunisienne dans son cadre méditerranéen. *Africa Geosciences Review*, 15, 3, 229-246.

Ben Slama, M.M., Masrouhi, A., Ghanmi, M., Zargouni, F., 2009. Albian extrusion evidences of Triassic salt and the clues of the beginning of the Eocene atlasic phase from the exemple of the Chitana Ed Djebs structure (N. Tunisia): implication in the North African Tethyan margin recorded events, comparisons. *Comptes Rendus Géosciences. 341, (7), 547-556.*

Bergerat, F., 1977. Le rôle des décrochements dans les liaisons tectoniques entre le Fossé de la Saône et le Fossé Rhénan. *Bulletin Société Géologique* France, 195-199.

Biju Duval, B., Dercourt, J., Le Pichon, X., 1977. From the Tethys ocean to the Mediterranean Sea: a plate tectonic model of the evolution of the western Alpine system. *Structural history of the western Mediterranean basins*, 143-164.

Bouaziz, S., Barrier, E., Soussi, M., Turki, M.M., Zouari, H., 2002. Tectonic evolution of the northern African margin in Tunisia from paleostress data and sedimentary record. *Tectonophysics*, 337, 227-253.

Boughdiri, M., Sallouhi, H., Maâlaoui, K., Soussi, M., Cordey, F., 2006. Calpionellid zonation of the Jurassic–Cretaceous transition in North-Atlasic Tunisia. Updated Upper Jurassic stratigraphy of the 'Tunisian trough' and regional correlations. *Comptes Rendus Geoscience* Paris, 338, 1250–1259

Boukadi, N., Bedir M., 1996. L'halocinèse en Tunisie: contexte tectonique et chronologique des évènements, *Comptes Rendus Académie Sciences* Paris, 322, IIa, 587-594.

Bousquet, J.C., Philip, H., 1986. Neotectonics of the tyrrenean Arc and Apennines: an example of evolution from Island to collisional stages. In the origin of arc. *Ed. C.F. Wezel, Elsevier*, 305-326.

Burollet, P. F., 1956. Contribution à l'étude stratigraphique de la Tunisie centrale, *Annales Mines et Géololgie* Tunis, 18, 350 p.

Carminati, E., Doglioni, C., 2004. Mediterranean Tectonics. *Encyclopedia of Geology, Elsevie*r, 1, 135–146.

Carminati, E., Wortel, M.J.R., Spakman, W., Sabadini, R., 1998. The role of slab detachment processes in the opening of the western–central mediterranean basins: some geological and geophysical evidence. *Earth Planet. Sci. Lett*. 160, 651–665.

Castany, G., 1948. Les fossés d'effondrements de Tunisie. *Annales Mines géologie Tunis*, 3, 126p.

Chihi, L., Philip, H., 1998. Les fossés de l'extrémité orientale du Maghreb (Tunisie et Algérie orientale) : tectonique mio-plio-quaternaire et implication dans l'évolution

géodynamique récente de la Méditerranée occidentale. *Notes Service Géologique. Tunisie*, 64, 103-116.

Dercourt, J., Zonenshain, L.P., Ricou, L.E., Kazmin, V.G., Le Pichon, X., Knipper, A.L., Grandjaquet, C., Sborshchikov, I.M., Boullin, J., Sorokhtin, O., Geyssant, J., Lepvrier, C., Biju Duval, B., Sibuet, J.C., Savostin, L.A., Westphal, M., Lauter, J.P., 1985. Présentation de 9 cartes paléogéographiques au 1/20000000 s'étendant de l'Atlantique au Pamir pour la période du Lias à l'Actuel. Bull. Soc. Géol. France 8, I, 5, 637-652.

Dlala, M., Chihi L., Ben Ayed, N., 1983. Evolution tectonique mio-plio-quaternaires du fossé de Kasserine (Tunisie centrale). Implication sur l'évolution géodynamique récente de la Tunisie. *Notes Service Géologique* Tunisie, 51, 57-72.

Doglioni, C., Harabaglia, P., Merlini, S., Mongelli, F., Peccerillo, A., Piromallo, C., 1999. Orogens and slabs vs. their direction of subduction. *Earth Sciences Reviews*, 45, 167–208.

Faccenna, C., Piromallo, C., Crespo-Blanc, A., Jolivet, L., Rossetti, F., 2004. Lateral slab deformation and the origin of the western Mediterranean arcs. *Tectonics* 23, 1012-1029.

Frizon de Lamotte, D., Leturmy, P., Missenard, Y., Khomsi, S., Ruiz, G., Saddiqi, O., Guillocheau, F., Michard, A., 2009. Mesozoic and Cenozoic vertical movements in the Atlas system (Algeria, Morocco, Tunisia): An overview. *Tectonophysics*, 475, 9–28.

Gharbi, R.A., Chihi, L., Hammami M., Abdelkader S. Kadri, A., 2005. Manifestations tectono-diapiriques synsédimentaires et polyphasages d'âge Crétacé supérieur-Quaternaire dans la région de Zag Et Tir (Tunisie centre-nord). *Comptes Rendus Géosciences*, Paris, 337, 14, 1293-1300.

Glangeaud, L., 1951. Interprétation tectono-physique des caractères structuraux et paléogéographiques de la Méditerranée occidentale. Bull. Soc. Géol. France 6, 735-762.

Granet, M., Judenherc, S., Souriau, A., 2000. Des images du système lithosphère-asthénosphère sous la France et leurs implications géodynamiques : l'apport de la tomographie télésismique et de l'anisotropie sismique. Bull. Soc. Géol. France, 149-167.

Hadj Sassi, M., Zouari, H., Jallouli, C., 2006. Contribution de la gravimétrie et de la sismique réflexion pour une nouvelle interprétation géodynamique des fossés d'effondrement en Tunisie : exemple du fossé de Grombalia. *Comptes Rendu Géosciences*, 338, 751–756.

Hurwitz, S., Garfunkel, Z., Ben-Gai, Y., Reznikov, M., Rotstein, Y., Gvirtzman, H., 2002. The tectonic framework of a complex pull-apart basin: seismic reflection observations in the Sea of Galilee, Dead Sea transform. *Tectonophysics*, 359, 289 – 306.

537 Jauzein, A., 1967. Contribution à l'étude géologique des confins de la dorsale tunisienne.
538 *Annales Minines Géologie*, Tunisie, 22, 475 p.
539 Letouzey, J., 1986. Cenozoic paleo-stress pattern in the Alpine Foreland and structural
540 interpretation in a platform basin. *Tectonophysics*, 132, 215-231.
541 Letouzey, J., Trémolière, P., 1980. Paleo-stress around the Mediterranean since the Mesozoic
542 from microtectonics: comparison with plate tectonics data. *Rock mechanism*, 9, 173-
543 192.
544 Masrouhi, A., Ghanmi, M., Ben Slama, M. M., Ben Youssef, M., Vila, J.M., Zargouni, F.,
545 2008. New tectono-sedimentary evidence constraining the timing of the positive
546 tectonic inversion and the Eocene Atlasic phase in northern Tunisia: Implication for the
547 North African paleo-margin evolution. Comtes Rendus Geoscience, 340, 771–778.
548 Meghraoui, M., A. Cisternas,, and H. Philip, (1986), Seismotectonics of the Cheliff basin:
549 Structural background of the El Asnam earthquake, Tectonics (Washington) 5, p.809-
550 836.
551 Mejri, F., Burollet, P.F., Ben Ferjani, A., 2006. *Petroleum geology of Tunisia*, mémoir de
552 l'ETAP, n°22, Tunisia, 233p.
553 Melki, F., Zouaghi, T., Ben Chelbi, M., Bedir, M., Zargouni, F., 2010. Tectono-sedimentary
554 events and geodynamic evolution of the Mesozoic and Cenozoic basins of the Alpine
555 Margin, Gulf of Tunis, north-easternTunisia offshore. *Comptes Rendus Geoscience*
556 342, 741–753.
557 Morgan, M.A., Grocott, J., Moody, R.T.J., 1998. The strucral evolution of the Zaghouan-
558 Ressas structural belt, northern Tunisia. *Geological Society*, London, Special
559 Publication, 132, 405-422.
560 Mzali, H., Zouari, H., 2006. Caractérisation géométrique et cinématique des structures liées
561 aux phases compressives de l'Éocène au Quaternaire inférieur en Tunisie : exemple de
562 la Tunisie nord-orientale *Comptes Rendus Geoscience* Paris, 338, 742–749.
563 Panza, G.F., Peccerillo, A., Aoudia, A. and Farina, B., 2007. Geophysical and petrological
564 modelling of the structure and composition of the crust and upper mantle in complex
565 geodynamic settings: The Tyrrhenian Sea and surroundings. *Earth-Science Reviews*, 80,
566 1–46.
567 Patriat, M., Ellouze, N., Deyb, Z., Gauliera, J.M., Ben Kilani, H., 2003. The Hammamet,
568 Gabe`s and Chotts basins (Tunisia): a review of the subsidence history. *Sedimentary*
569 *Geology* 156, 241–262.

570 Perthuisot, V., Jauzein, A., 1974. L'accident El Alia-Tébessa dans la région de Téboursouk.
571 *Notes Service Géologique* Tunisie, 9, 57-63.
572 Perthuisot, V., Aoudjehane, M., Bouzenoune, A., Hatira, N., Laatar E., Mansouri A., Rouvier
573 H., Smati A., Thibiéroz J., 1998. Les corps triasiques des monts du Mellègue (confins
574 algéro-tunisiens) sont-ils des diapirs ou des «Glaciers de sel»?, Bull. Soc. Géol. France
575 169, 53-61.
576 Philip, H., Andrieux, J., Dlala, M., Chihi, L., Ben Ayed, N., 1986. Evolution tectonique mio-
577 plio-quaternaire du fossé de Kasserine (Tunisie centrale): implications sur l'évolution
578 géodynamique récente de la Tunisie. Bull. Soc. Géol. France 4, 559-568.
579 Piqué, A., Ait Brahim, L., Ait Ouali, R., Amrhar, M., Charroud, F., Gourmelen, C., Laville,
580 E., Rekhiss, F., Tricart, P., 1998. Evolution structurale des domaines atlasique du
581 Maghreb au Méso-Cénozoïque; le rôle des structures héritées dans la déformation du
582 domaine atlasique de l'Afrique de Nord. Bull. Soc. Géol. France 169, 6 797-810.
583 Rebai, S., Philip, H., Taboada A., 1992. Modern tectonic stress field in the Mediterranean
584 region: evidence for variation in stress directions at different scales, *Geophys. J. Int.*
585 110, 106-140.
586 Richet, J.P., 1971. Mise en évidence de quatre phases tectoniques successives en Tunisie.
587 *Note Service Géologique* Tunisie, N° 34, 115-125.
588 Ricou, L. E., 1994. Tethys reconstructed: plates, continental fragments and their boundaries
589 since 260Ma from Central America to South Asia. *Géodynamica Acta*, 7, 160-218.
590 Rosendahl, B. R., 1987, Architecture of continental rifts with special reference to East Africa:
591 Annual Review of Earth and Planetary Science, v. 15, p. 445-503.
592 Saidia, A., Tahiria, A., Ait Brahimb, L., Saidia, M., 2002. États de contraintes et mécanismes
593 d'ouverture et de fermeture des bassins permiens du Maroc hercynien. L'exemple des
594 bassins des Jebilet et des Réhamna. *Comptes Rendu Géosciences,* 334, 221–226.
595 Sekatni, N., Fauré, Ph., Alouani, R., Zargouni, F., 2008. Le passage Lias–Dogger de la
596 Dorsale de Tunisie septentrionale Nouveaux apports biostratigraphiques. Âge Toarcien
597 supérieur de la distension téthysienne, *Comptes Rendus Palevol,* 7, 185–194.
598 Schlische, R.W. and Withjack, M.O., 1999, Report on the International Workshop for a
599 Climatic, Biotic, and Tectonic, Pole-to-Pole Coring Transect of Triassic-Jurassic
600 Pangea Held June 5-9, 1999 at Acadia University, Nova Scotia, Canada.
601 Snoke, A., Schamel S., Karasek R., 1988. Structural evolution of the Jebel Debadib anticline: a
602 clue to the regional tectonic style of the Tunisian Atlas. *Tectonophysics* 7, 497-516.

603 Soussi, M., Ben Ismaïl, M.H. 2000. Platform collapse and pelagic seamount facies: Jurassic
604 development of central Tunisia. *Sedimentary Geology*, 133, 93–113
605 Soussi, M., 2003. New Jurassic lithostratigraphic chart for the Tunisian atlas. *Geobios* 36
606 761–773.
607 Soyer, C., Tricart, P., 1987. La crise aptienne en Tunisie central: approche paléostructurale
608 aux confins de l'Atlas et de l'Axe Nord-Sud. *Comptes Rendus de l'Académie des*
609 *Sciences* Paris, 305, II, 301-305.
610 Talbi, F., Melki, F., Ben Ismail-Lattrache, K., Alouani, R., Tlig, S., 2008. Le Numidien de la
611 Tunisie septentrionale: données stratigraphiques et interprétation géodynamique
612 *Estudios Geológicos*, 64, 131-144.
613 Tapponnier, P., 1977. Evolution tectonique du système alpin en méditerranée: poinçonnement
614 et écrasement rigide-plastique. Bull. Soc. Géol. France 19, 3, 437-460.
615 Tlig, S., Er-Raoui, L., Ben Aissa, L., Alouani, R., Tagorti, M.A., 1991. Tectogenèses alpine et
616 atlasique : deux évènements distincts dans l'histoire géologique de la Tunisie.
617 Corrélation avec les évènements clés de la Méditerranée. *Comptes Rendus Académie de*
618 *Sciences* Paris, t.312, II, 295-301.
619 Vila, J.M., Ben Youssef, M., Charrière, A., Chikhaoui, M., Ghanmi, M., Kammoun, F.,
620 Peybernès, B., Saadi, J., Souquet, P., Zarbout, M., 1994. Découverte en Tunisie au SW
621 du Kef de matériel triasique interstratifié dans l'Albien: extension du domaine à
622 «glacier de sel» sous-marin des confins algéro-tunisiens. *Comptes Rendus Académie de*
623 *Sciences* Paris, 318, II 109-116.
624 Zouari, H., Turki, M.M., Delteil, J., Stephan, J.F., 1999. Tectonique transtensive de la
625 paléomarge tunisienne au cours de l'Aptien-Campanien. Bull. Soc. Géol. France 170, 3,
626 295-301.
627
628
629
630
631
632
633
634
635
636

Figure captions

Fig. 1: A- Simplified structural map of the northern and central Tunisian Atlas and localization of the studied area (T2: Zaghouan Fault, T3: Tunis-Ellès fault, T4: El Alia-Teboursouk Fault; After Melki et al. 2010). **B-** Structural zoning of Tunisia showing the structural position of the Bou Arada Trough (After Ben Chelbi et al. 2008).

Fig. 2: A- Geomorphologic context of the studied area (SRTM 30m). **B-** Geologic map of the studied area (1- Triassic; 2- Early Cretaceous; 3- Late Cretaceous; 4- Campanian-Maastrichtian; 5- Palaeocene-Middle Eocene; 6- Late Eocene-Oligocene-Aquitanian; 7- Mio-Pliocene; 8- Quaternary; 9: Fault; 10: Localization of the seismic lines; 11: Localization of the cross sections).

Fig 3: Lithostratigraphic column of the study area

Fig. 4: Synthetic chart of the geodynamics of the Tunisian Atlas showing the relationship between convergence tectonics and salt tectonics, after Patriat et al. (2003), Mejri et al. (2006), and Ben Chelbi et al. (2008). Arrows are oriented with respect to the North as a vertical direction.

Fig. 5: Geological cross sections (for localization see Fig. 3C) showing the northernmost contacts of the graben of Bou Arada with the neighbouring structures (**Apt**.: Aptian; **Alb.:** Albian; **Cen**.: Cenomanian; **Con.**: Coniacian; **Sant**.: Santonian; **Maast.:** Maastrichtian; **La. Eoc.**: Late Eocene; **Olig.**: Oligocene; **Mio-Plio**.: Mio-Pliocene; **Q.**: Quaternary)

Fig. 6: Geological cross sections showing the southernmost contacts of the Bou Arada Trough with the neighbouring structures (see Figs 2B and 5 for locations). Abbreviations denote: **Apt**., Aptian; **Alb**., Albian; **Cen**., Cenomanian; **Con.**, Coniacian; **Sant**., Santonian; **Camp.**, Campanian; **Maast.**, Maastrichtian; **Ea. Eoc.**, Early Eocene; **La**. **Eoc.**, Late Eocene; **Olig**., Oligocene; **Ea. Olig.**, Early Oligocene; **La**. **Olg.**, Late Oligocene; **Mio-Plio.**, Mio-Pliocene; **Mio-Plio-Q**., Mio-Plio-Quaternary; and **Q.**, Quaternary.

Fig. 7: Raw (**P1, P2**) and interpreted (**P'1, P'2**) N-S oriented seismic lines showing the configuration and the geometry of the Bou Arada Trough (see Fig. 2B for locations). Fine

lines denote limits of formations, thicker lines denote faults, and broken lines denote limits of Triassic series. Abbreviations denote: **M.P.Q**., Mio-Plio-Quaternary; **Ol.Aq.,** Oligo-Aquitnian; **E.3,** Late Eocene; **M.E.2,** Maastrichtian to middle Eocene; **Co.Ca**., Coniacian to Campanian; **Al.Tur**., Albian-Turonian.

Fig. 8: Raw (**P3, P4**) and interpreted (**P'3, P'4**) E-W and NW-SE oriented seismic lines showing the configuration and the geometry of the Bou Arada Trough (see Fig. 2B for locations). Notation is the same as for Fig. 7.

Fig. 9: Correlation proposed in this study between the lithostraigraphic series on both sides of the Bou Arada Trough (A, B, C) showing modes of formation (A', B', C') and the evolution of this trough since the Campanian.

Fig. 10: Evolution of the Bou Arada Trough in response to the various tectonic constraints during Maastrichtian- middle Eocene. **A** depicts a stereographic representation (Schmidt's projection, lower hemisphere) of the various populations of faults affecting the different layers in studied area (continuous lines); a strike rose diagram, showing principal stress axes orientation and value (**σ1, σ2 and σ3**)). **B** depicts interpretations of the stereograms showing the various activities recorded on major faults. **C** depicts schematic block diagram showing the paleostructuration of the studied area (⇦ ⇨ extension regime, ➡⬅ Compression regime). **D** depicts an evolutionary model of BAT in relation to the bordering system of faults).

Fig. 11: Evolution of the Bou Arada Trough in response to the various tectonic constraints during Late Eocene-Aquitanien (same legend as Fig. 11).

Fig. 12: Evolution of the Bou Arada Trough in response to the various tectonic constraints during Middle to Late Miocene (same legend as Fig. 11).

Fig. 13: Evolution of the Bou Arada Trough in response to the various tectonic constraints during Late Miocene-Pliocene (same legend as Fig. 11).

Fig. 14: Evolution of the Bou Arada Trough in response to the various tectonic constraints during Quaternary-Actual (same legend as Fig. 11).

Fig. 15: A) Block diagram schematically showing the pull-apart model of formation of the BAT during transpression. **B)** Simplified sketch showing the faults that controlled the evolution of the BAT.

Table 1: Synthetic table of the palaeostress data used for the reconstruction of the tectonic evolution of the study area Tunisia (**N:** number of fault plans; **σ1, σ2, σ3:** Direction and value of the stress; **Φ:** ratio of stress magnitude differences (**Φ = σ2-σ3/σ1-σ3**); **R:** Palaeostress regimes; **C**, **E**, **TT** and **TP**: Compressional, Extensional, Transtensive and Transpressive regimes, respectively.

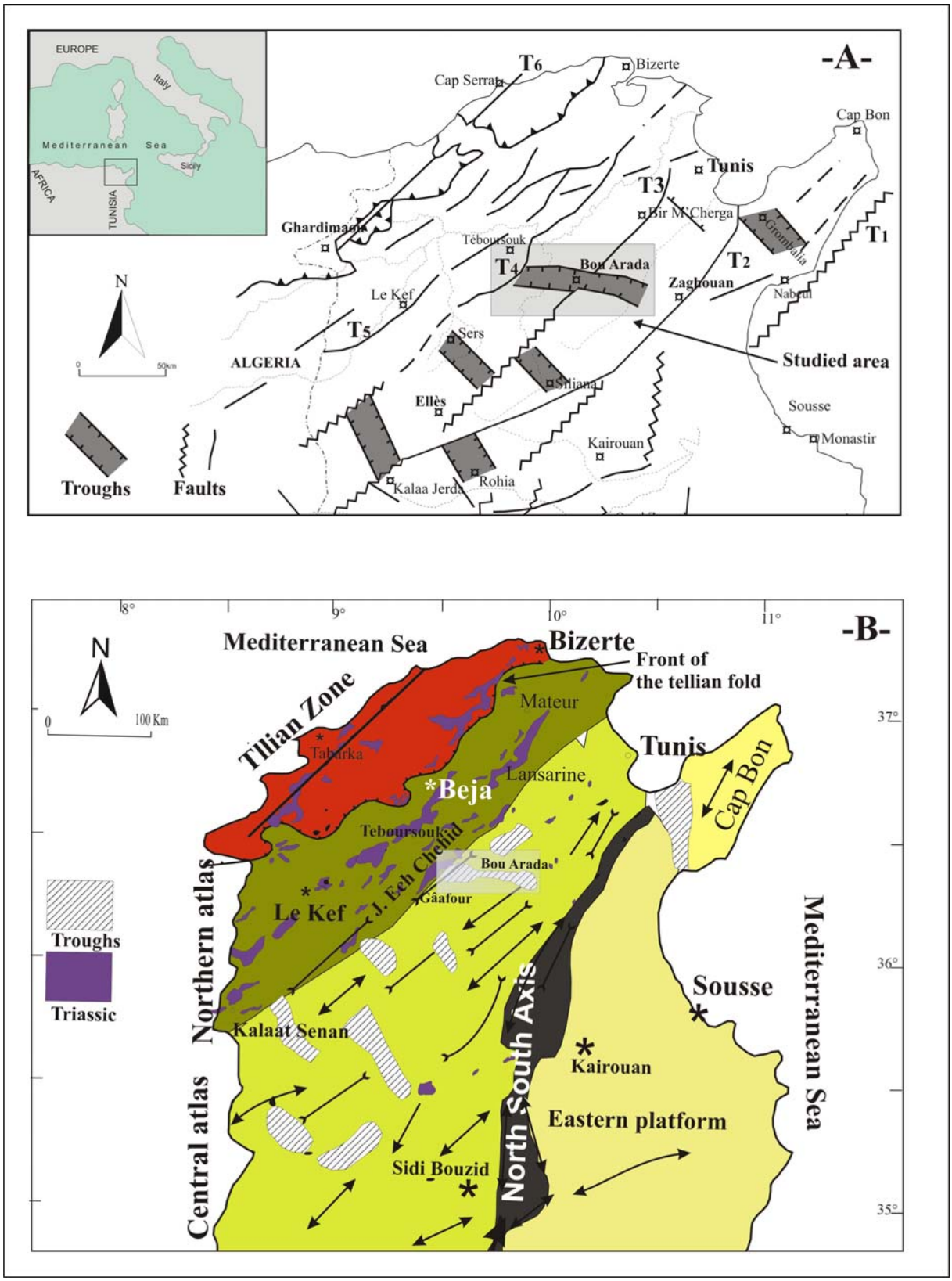
-A-
EUROPE
Italy
Mediterranean Sea
Sicily
AFRICA
TUNISIA
N
0
50km
ALGERIA
Troughs
Faults
T6
Cap Serrat
Bizerte
Cap Bon
Tunis
T3
Bir M'Cherga
Grombalia
T1
T2
Ghardimaou
Téboursouk
T4
Bou Arada
Zaghouan
Nabeul
Le Kef
T5
Sers
Studied area
Siliana
Ellès
Sousse
Monastir
Kairouan
Kalaa Jerda
Rohia
-B-
8°
9°
10°
11°
37°
36°
35°
N
0
100 Km
Mediterranean Sea
Bizerte
Front of
the tellian fold
Mateur
Tlian Zone
Tabarka
Tunis
Cap Bon
*Beja
Lansarine
Téboursouk
Bou Arada
J. Ech Chelid
Gâafour
Le Kef
Troughs
Triassic
Northern atlas
Sousse
Kalaat Senan
Kairouan
North South Axis
Eastern platform
Mediterranean Sea
Central atlas
Sidi Bouzid

Fig.1:

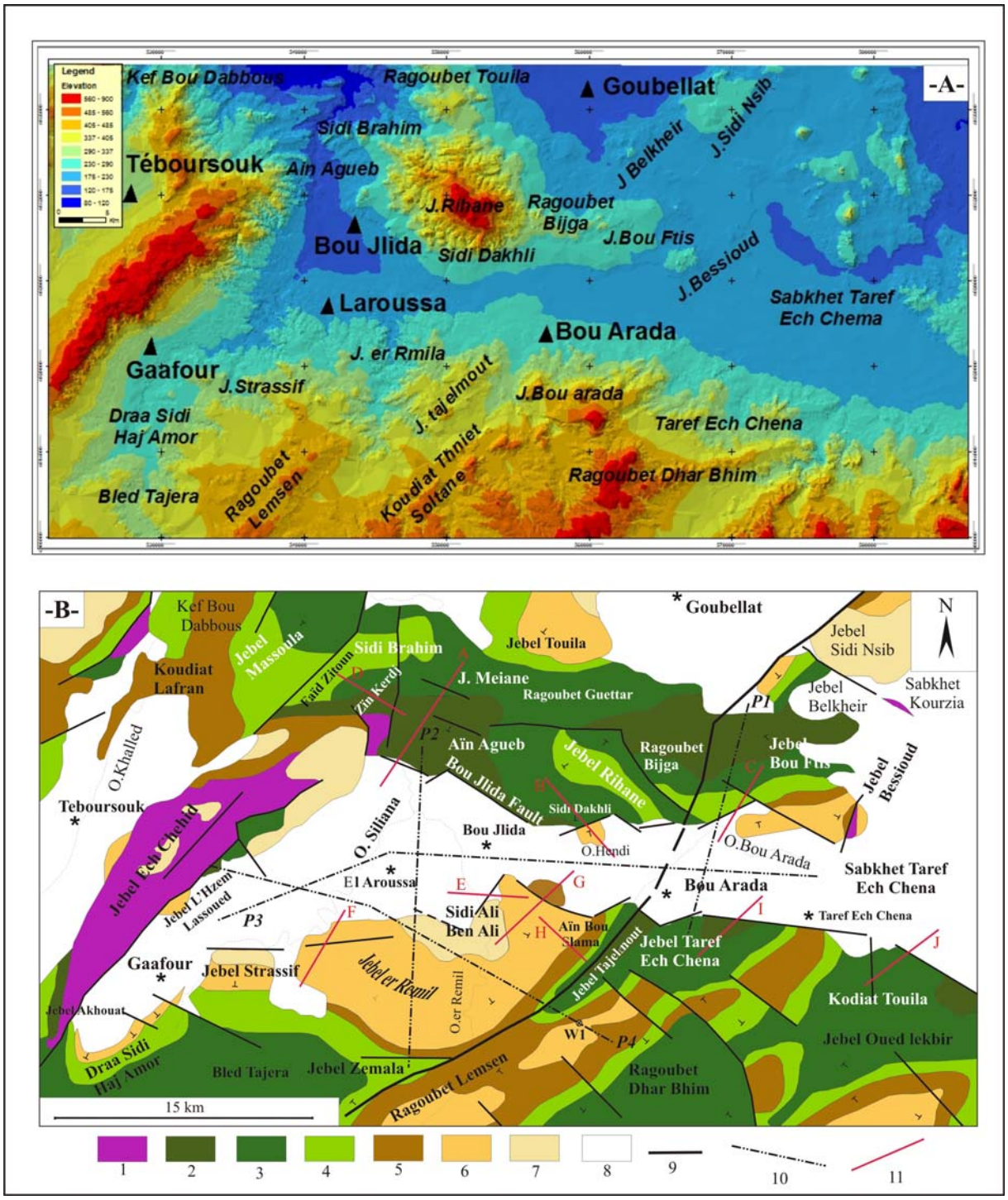
-A-
Legend
Elevation
Kef Bou Dabbous
Ragoubet Touila
Goubellat
Sidi Brahim
Téboursouk
Ain Agueb
J Belkheir
J.Sidi Nsib
J.Rihane
Ragoubet Bijga
Bou Jlida
Sidi Dakhli
J.Bou Ftis
J.Bessioud
Laroussa
Sabkhet Taref Ech Chema
Bou Arada
Gaafour
J. er Rmila
J.Strassif
J. tajelmout
J.Bou arada
Draa Sidi Haj Amor
Taref Ech Chena
Bled Tajera
Ragoubet Lemsen
Koudiat Thniet Soltane
Ragoubet Dhar Bhim
-B-
Kef Bou Dabbous
Jebel Massouda
Goubellat
Jebel Touila
Jebel Sidi Nsib
N
Koudiat Lafran
Faid Zitoun
Sidi Brahim
Zin Kerdj
J. Meiane
Ragoubet Guettar
Jebel Belkheir
Sabkhet Kourzia
P1
P2
O.Khalled
Aïn Agueb
Jebel Rihane
Ragoubet Bijga
Jebel Bou Ftis
Jebel Bessioud
Teboursouk
Bou Jlida Fault
Sidi Dakhli
Jebel Ech Chehid
O. Siliana
Bou Jlida
O.Hendi
O.Bou Arada
Sabkhet Taref Ech Chena
El Aroussa
Bou Arada
Jebel L'Hzem Lassoued
P3
Sidi Ali Ben Ali
Taref Ech Chena
Aïn Bou Slama
Gaafour
Jebel Strassif
Jebel er Remil
Jebel Tajelmout
Jebel Taref Ech Chena
Kodiat Touila
Jebel Akhouat
O.er Remil
W1
P4
Jebel Oued lekbir
Draa Sidi Haj Amor
Bled Tajera
Jebel Zemala
Ragoubet Lemsen
Ragoubet Dhar Bhim
15 km
1
2
3
4
5
6
7
8
9
10
11

Fig.2:

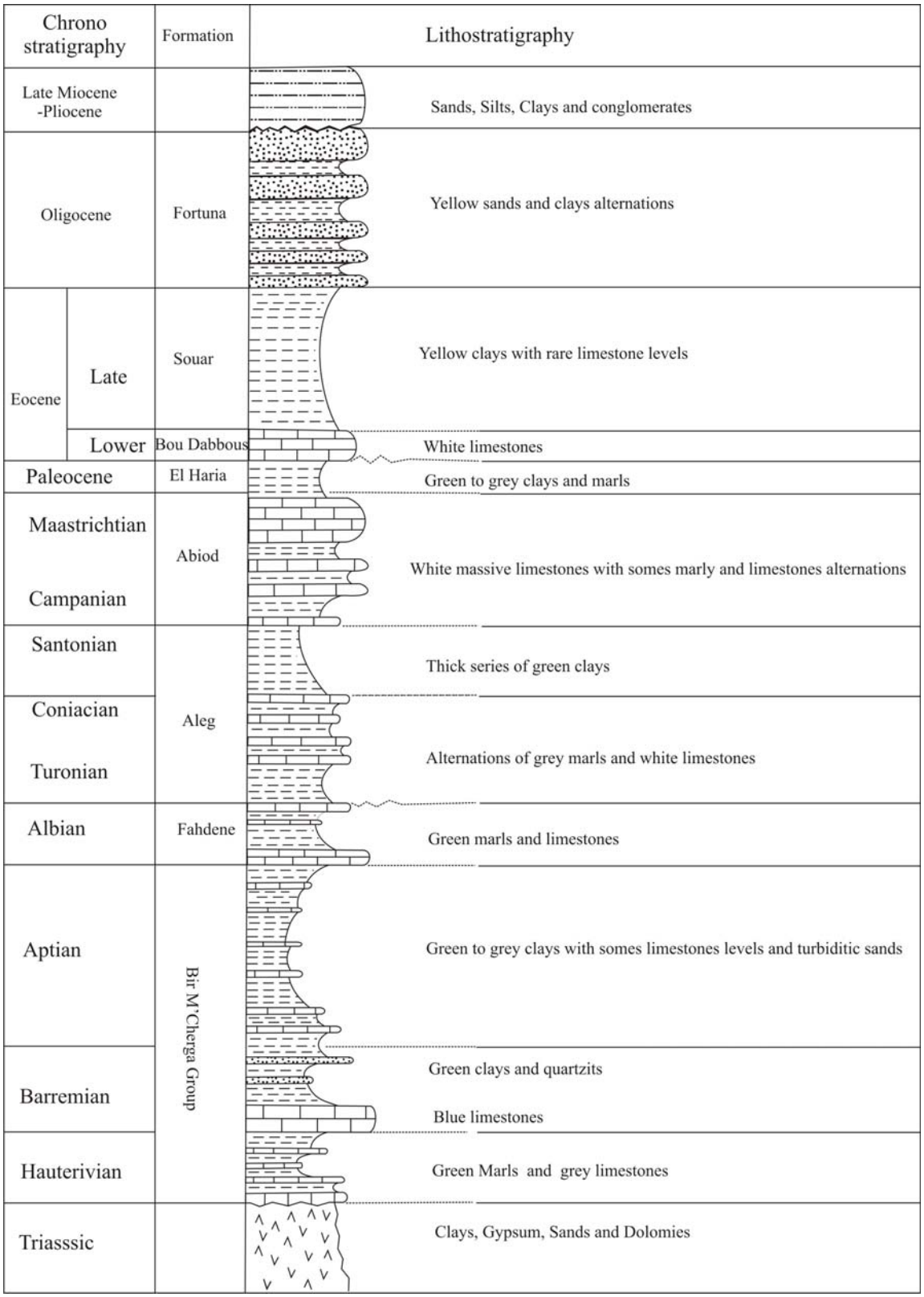
Chrono stratigraphy
Formation
Lithostratigraphy
Late Miocene -Pliocene
Sands, Silts, Clays and conglomerates
Oligocene
Fortuna
Yellow sands and clays alternations
Eocene
Late
Souar
Yellow clays with rare limestone levels
Lower
Bou Dabbous
White limestones
Paleocene
El Haria
Green to grey clays and marls
Maastrichtian
Campanian
Abiod
White massive limestones with somes marly and limestones alternations
Santonian
Thick series of green clays
Coniacian
Turonian
Aleg
Alternations of grey marls and white limestones
Albian
Fahdene
Green marls and limestones
Aptian
Green to grey clays with somes limestones levels and turbiditic sands
Barremian
Green clays and quartzits
Blue limestones
Hauterivian
Bir M'Cherga Group
Green Marls and grey limestones
Triasssic
Clays, Gypsum, Sands and Dolomies

Fig.3:

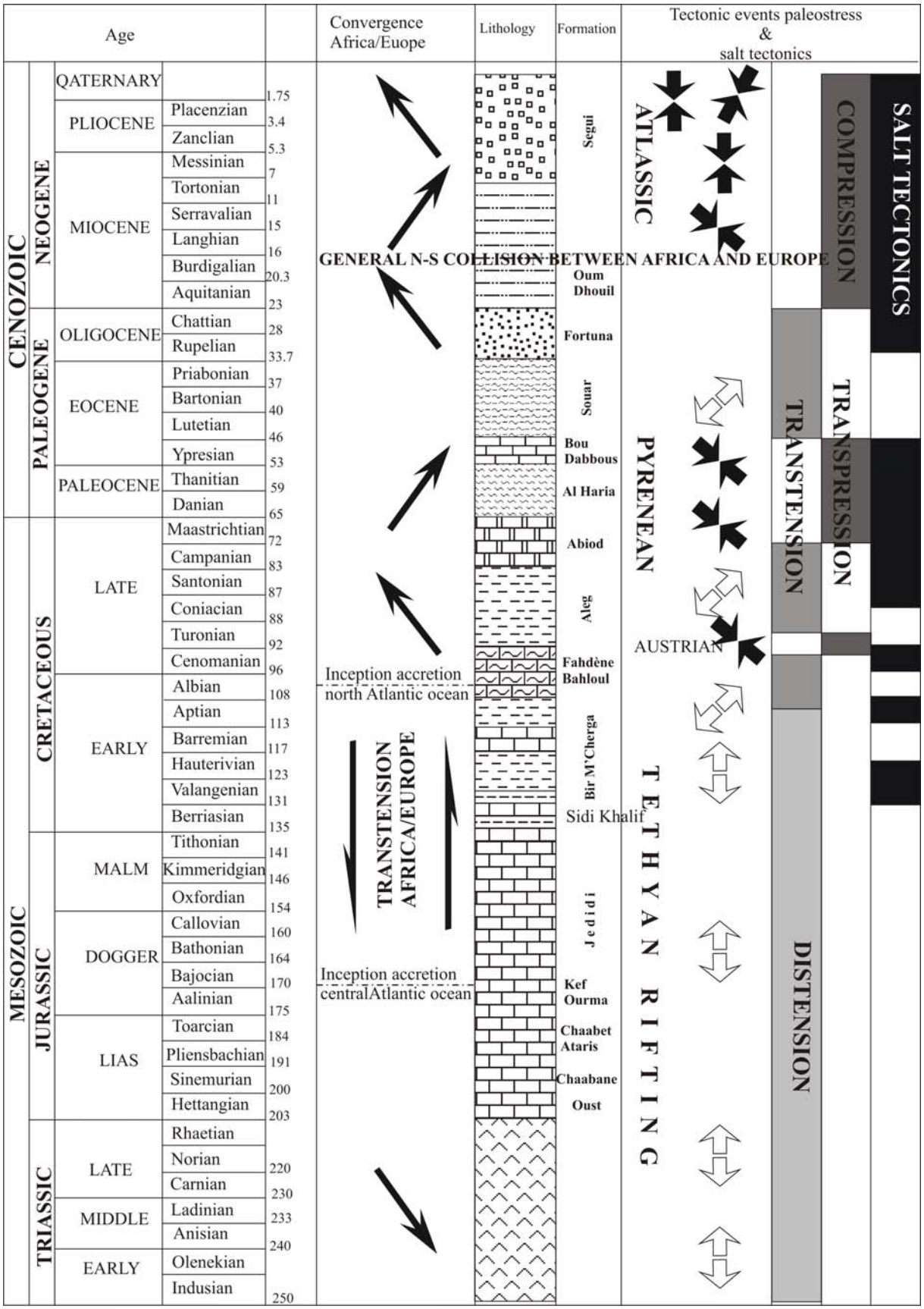
Age
Convergence Africa/Euope
Lithology
Formation
Tectonic events paleostress & salt tectonics
CENOZOIC
MESOZOIC
NEOGENE
PALEOGENE
CRETACEOUS
JURASSIC
TRIASSIC
QATERNARY
PLIOCENE
MIOCENE
OLIGOCENE
EOCENE
PALEOCENE
LATE
EARLY
MALM
DOGGER
LIAS
MIDDLE
Placenzian
Zanclian
Messinian
Tortonian
Serravalian
Langhian
Burdigalian
Aquitanian
Chattian
Rupelian
Priabonian
Bartonian
Lutetian
Ypresian
Thanitian
Danian
Maastrichtian
Campanian
Santonian
Coniacian
Turonian
Cenomanian
Albian
Aptian
Barremian
Hauterivian
Valangenian
Berriasian
Tithonian
Kimmeridgian
Oxfordian
Callovian
Bathonian
Bajocian
Aalinian
Toarcian
Pliensbachian
Sinemurian
Hettangian
Rhaetian
Norian
Carnian
Ladinian
Anisian
Olenekian
Indusian
1.75
3.4
5.3
7
11
15
16
20.3
23
28
33.7
37
40
46
53
59
65
72
83
87
88
92
96
108
113
117
123
131
135
141
146
154
160
164
170
175
184
191
200
203
220
230
233
240
250
GENERAL N-S COLLISION BETWEEN AFRICA AND EUROPE
Inception accretion north Atlantic ocean
TRANSTENSION AFRICA/EUROPE
Inception accretion centralAtlantic ocean
Segui
Oum Dhouil
Fortuna
Souar
Bou Dabbous
Al Haria
Abiod
Aleg
Fahdène Bahloul
Bir M'Cherga
Sidi Khalif
Jedidi
Kef Ourma
Chaabet Ataris
Chaabane
Oust
ATLASSIC
PYRENEAN
AUSTRIAN
TETHYAN RIFTING
SALT TECTONICS
COMPRESSION
TRANSPRESSION
TRANSTENSION
DISTENSION

Fig.4:

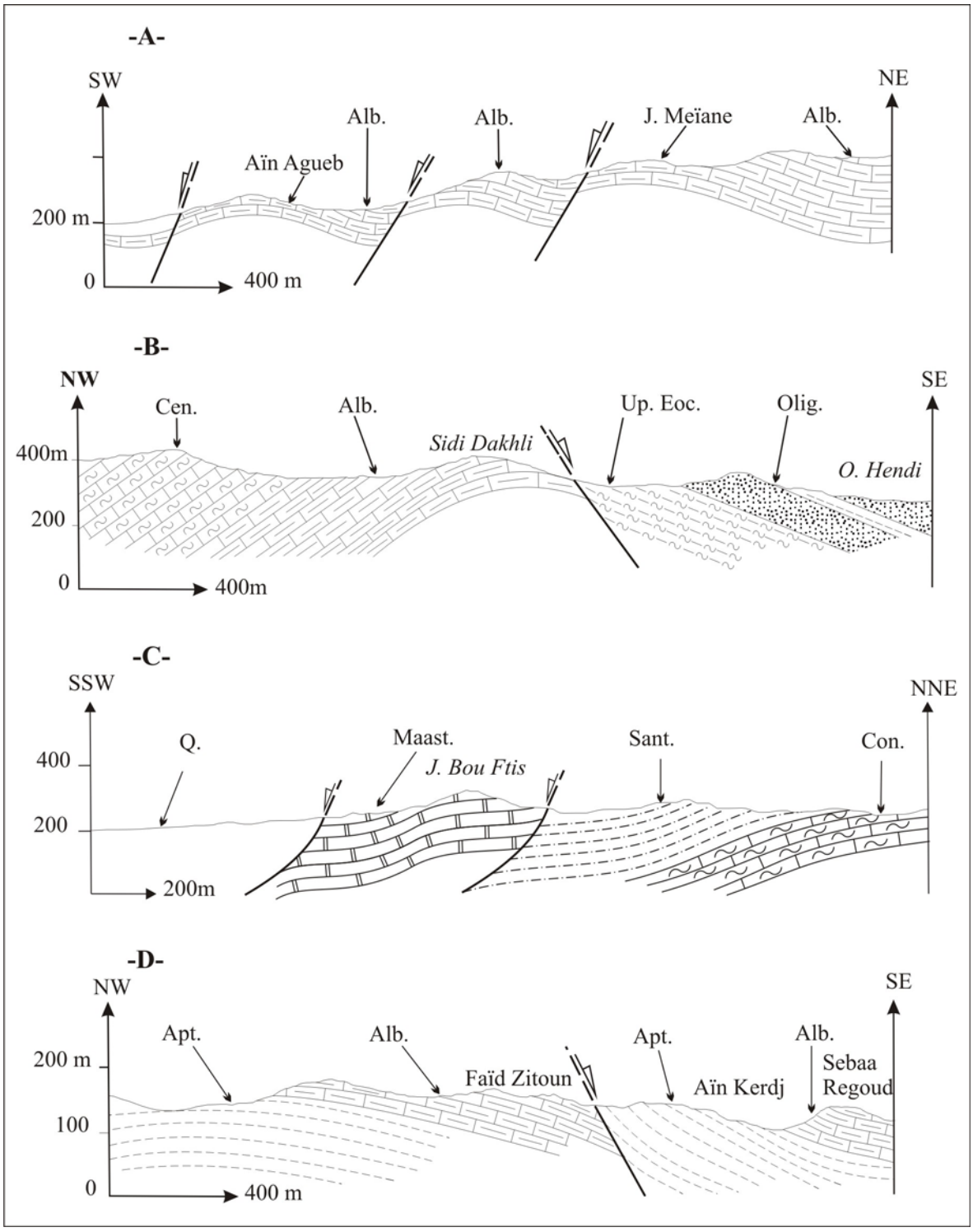
-A-
SW
NE
Alb.
Alb.
J. Meïane
Alb.
Aïn Agueb
200 m
0
400 m
-B-
NW
SE
Cen.
Alb.
Up. Eoc.
Olig.
Sidi Dakhli
O. Hendi
400m
200
0
400m
-C-
SSW
NNE
Q.
Maast.
J. Bou Ftis
Sant.
Con.
400
200
200m
-D-
NW
SE
Apt.
Alb.
Apt.
Alb.
Sebaa
Regoud
Faïd Zitoun
Aïn Kerdj
200 m
100
0
400 m

Fig.5:

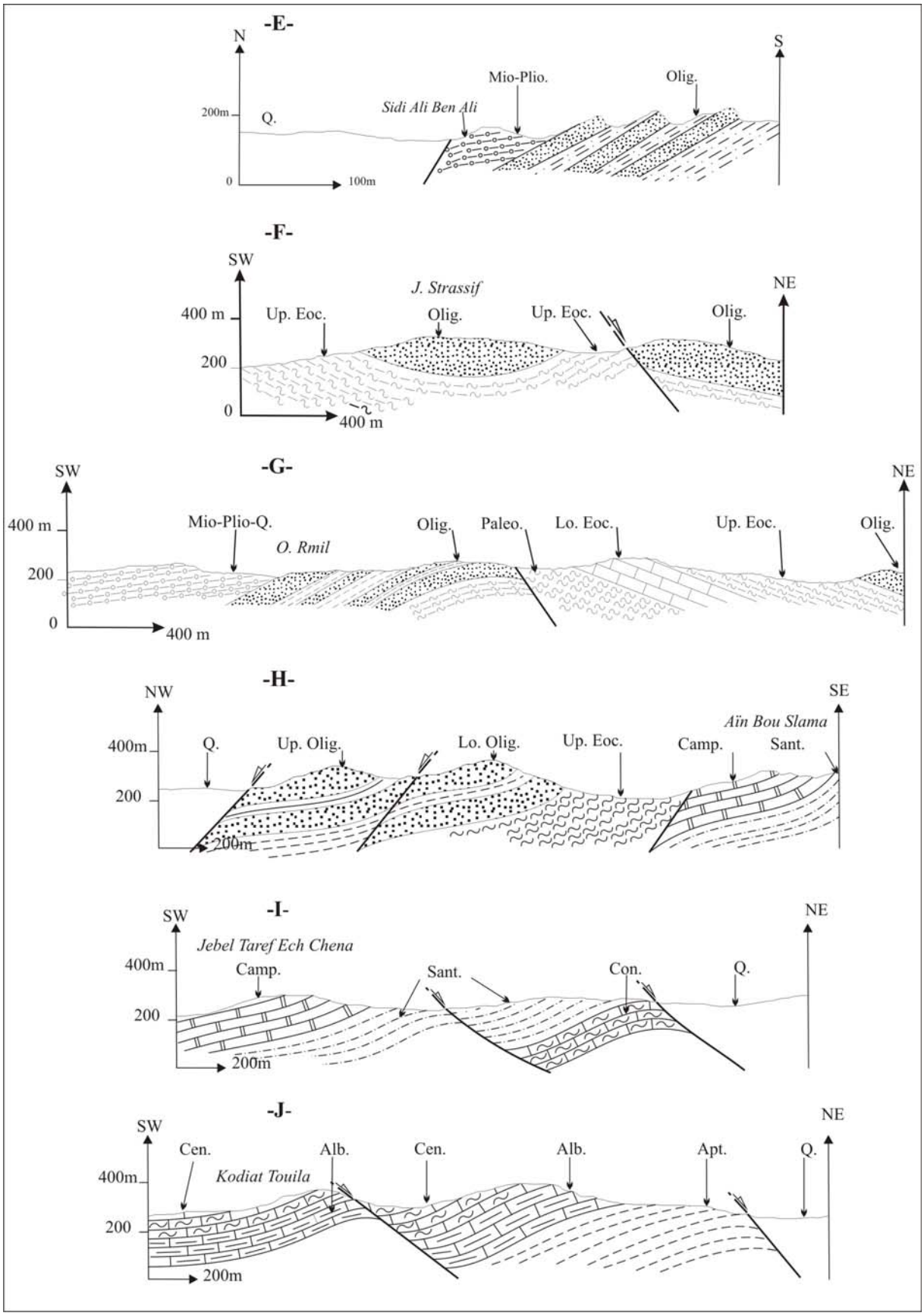
-E-
N
S
Mio-Plio.
Olig.
Sidi Ali Ben Ali
200m
Q.
0
100m
-F-
SW
NE
J. Strassif
400 m
Up. Eoc.
Olig.
Up. Eoc.
Olig.
200
0
400 m
-G-
SW
NE
400 m
Mio-Plio-Q.
Olig.
Paleo.
Lo. Eoc.
Up. Eoc.
Olig.
O. Rmil
200
0
400 m
-H-
NW
SE
Aïn Bou Slama
400m
Q.
Up. Olig.
Lo. Olig.
Up. Eoc.
Camp.
Sant.
200
200m
-I-
SW
NE
Jebel Taref Ech Chena
400m
Camp.
Sant.
Con.
Q.
200
200m
-J-
SW
NE
Cen.
Alb.
Cen.
Alb.
Apt.
Q.
400m
Kodiat Touila
200
200m

Fig.6:

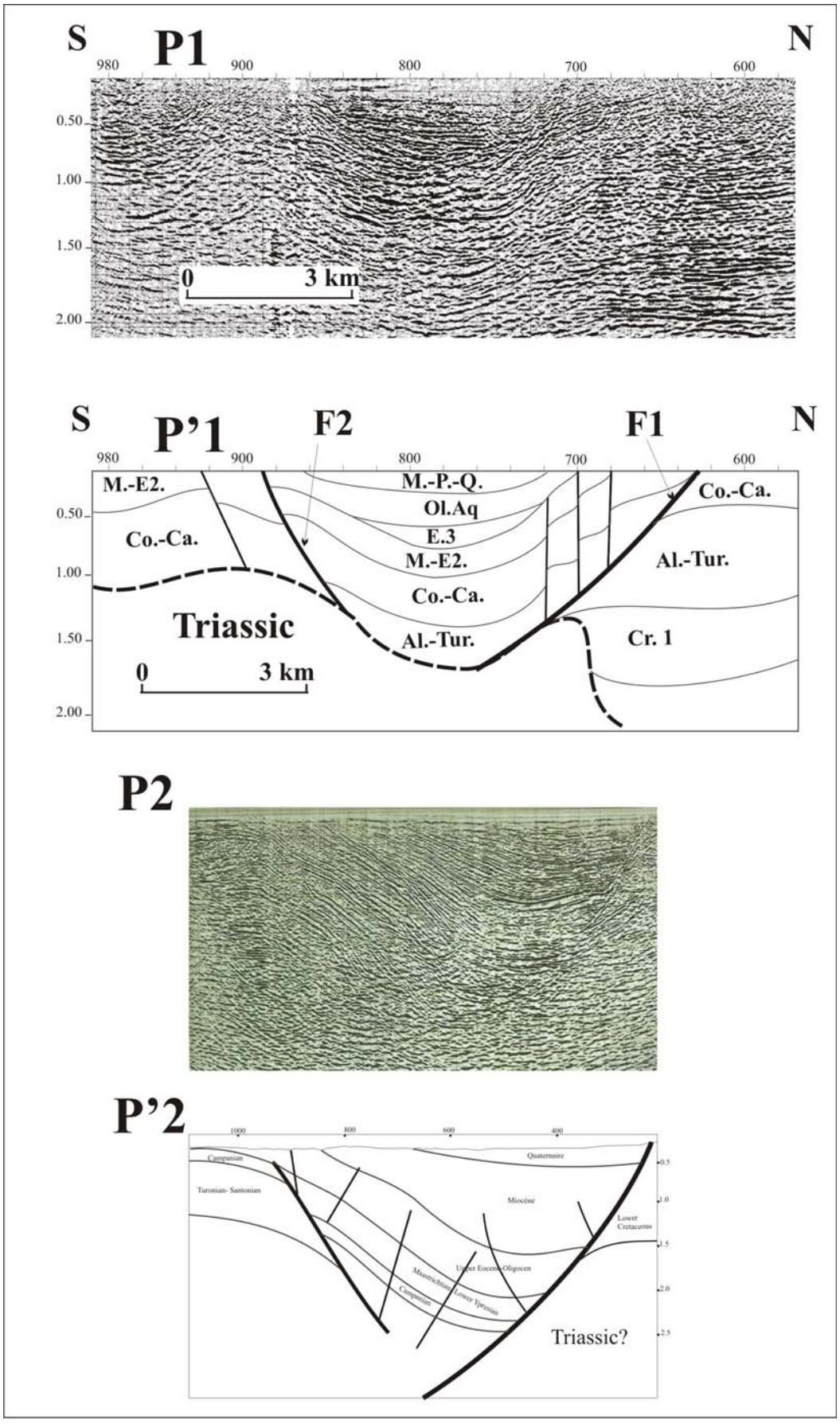
S
P1
N
980
900
800
700
600
0.50
1.00
1.50
2.00
0
3 km
S
P'1
F2
F1
N
980
900
800
700
600
M.-E2.
Co.-Ca.
M.-P.-Q.
Ol.Aq
E.3
M.-E2.
Co.-Ca.
Al.-Tur.
Co.-Ca.
Al.-Tur.
Triassic
Cr. 1
0
3 km
P2
P'2
1000
800
600
400
Campanian
Quaternaire
Turonian- Santonian
Miocène
Lower Cretaceous
Upper Eocene-Oligocen
Maastrichtian-Lower Ypresian
Campanian
Triassic?

770

771 Fig. 7:

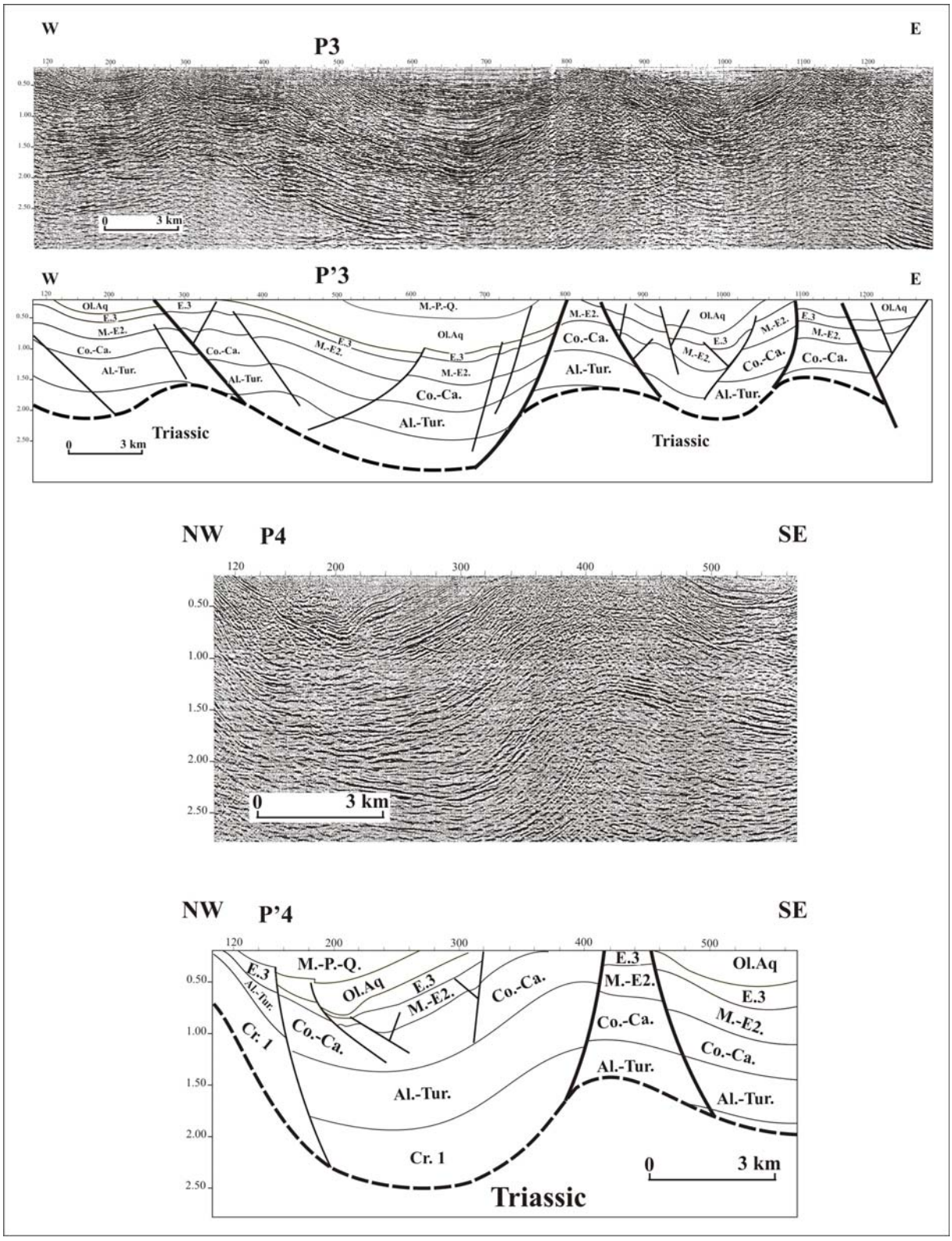
W
E
P3
0
3 km
W
P'3
E
Ol.Aq
E.3
M.-E2.
Co.-Ca.
Al.-Tur.
M.-P.-Q.
Triassic
0
3 km
NW
P4
SE
0
3 km
NW
P'4
SE
Cr. 1
Triassic
0
3 km

Fig. 8:

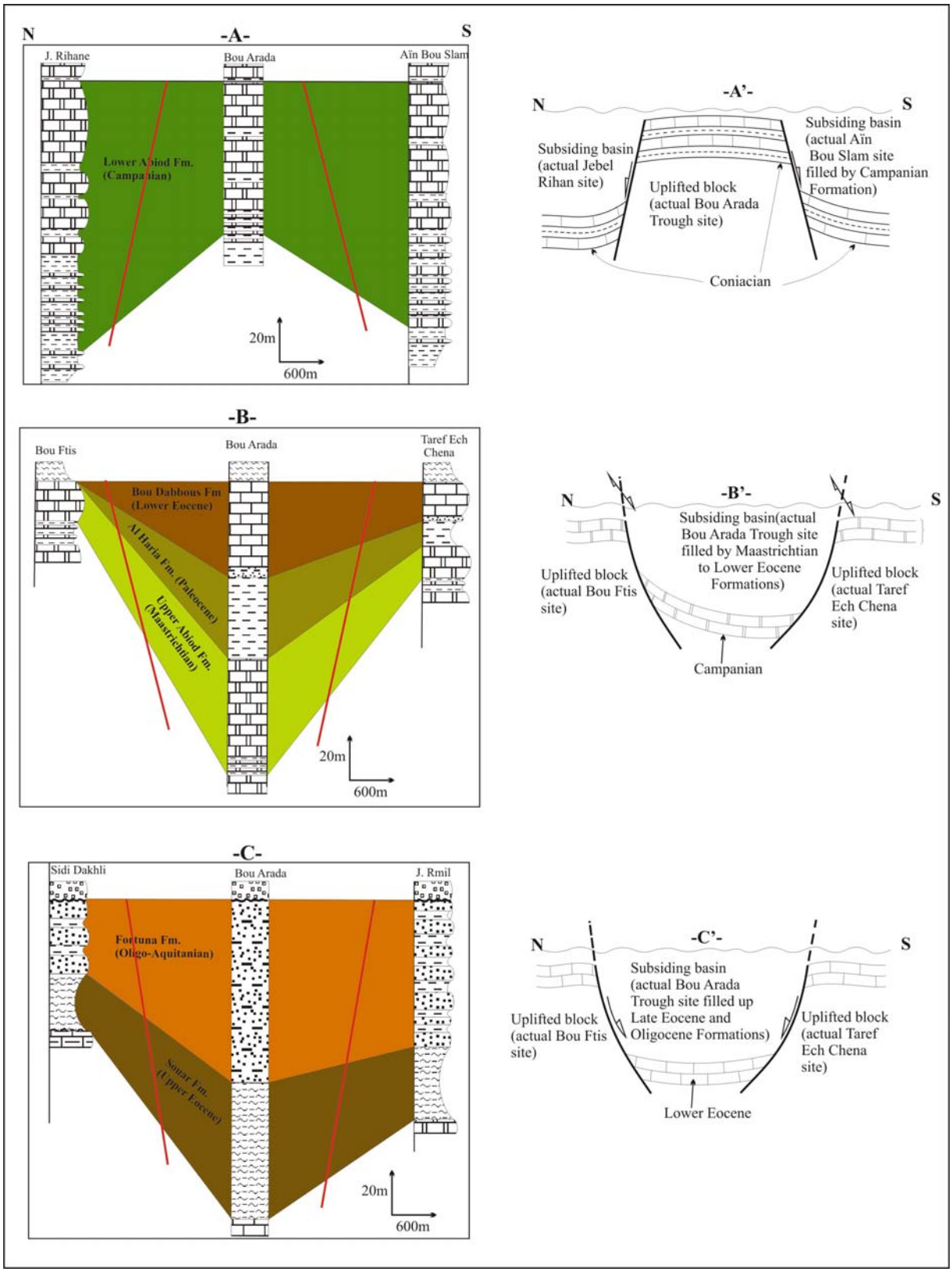
N
-A-
S
J. Rihane
Bou Arada
Aïn Bou Slam
Lower Abiod Fm.
(Campanian)
20m
600m
-A'-
N
S
Subsiding basin
(actual Jebel
Rihan site)
Uplifted block
(actual Bou Arada
Trough site)
Subsiding basin
(actual Aïn
Bou Slam site
filled by Campanian
Formation)
Coniacian
-B-
Bou Ftis
Bou Arada
Taref Ech
Chena
Bou Dabbous Fm
(Lower Eocene)
Al Haria Fm. (Paleocene)
Upper Abiod Fm.
(Maastrichtian)
20m
600m
-B'-
N
S
Subsiding basin(actual
Bou Arada Trough site
filled by Maastrichtian
to Lower Eocene
Formations)
Uplifted block
(actual Bou Ftis
site)
Uplifted block
(actual Taref
Ech Chena
site)
Campanian
-C-
Sidi Dakhli
Bou Arada
J. Rmil
Fortuna Fm.
(Oligo-Aquitanian)
Souar Fm.
(Upper Eocene)
20m
600m
-C'-
N
S
Subsiding basin
(actual Bou Arada
Trough site filled up
Late Eocene and
Oligocene Formations)
Uplifted block
(actual Bou Ftis
site)
Uplifted block
(actual Taref
Ech Chena
site)
Lower Eocene

Fig. 9:

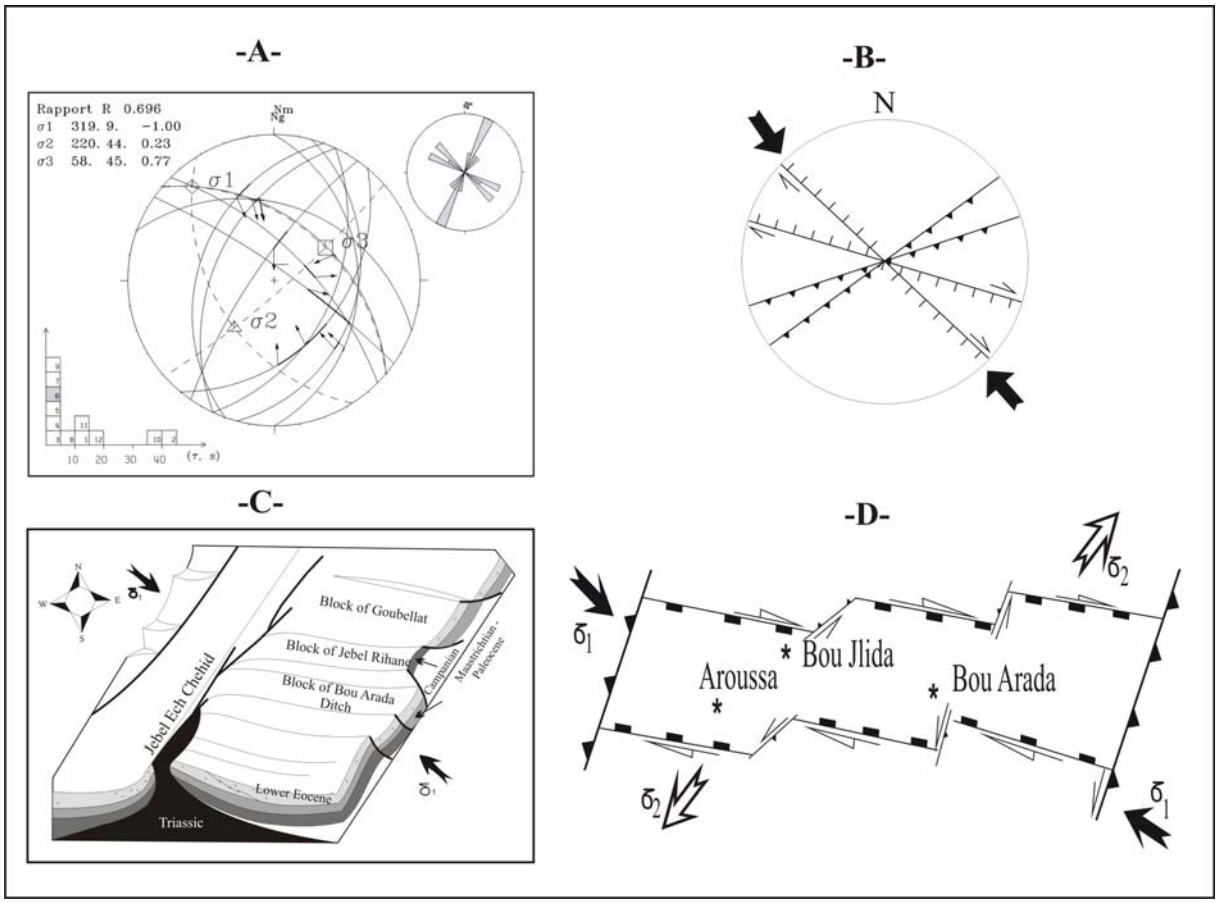
-A-
Rapport R 0.696
σ1 319. 9. -1.00
σ2 220. 44. 0.23
σ3 58. 45. 0.77
Nm
Ng
σ1
σ2
σ3
10 20 30 40 (τ. s)
-B-
N
-C-
N
E
S
W
σ1
Jebel Ech Chehid
Block of Goubellat
Block of Jebel Rihane
Block of Bou Arada Ditch
Campanian
Maastrichtian - Paleocene
Lower Eocene
Triassic
σ1
-D-
σ2
σ1
Aroussa
Bou Jlida
Bou Arada
σ2
σ1

Fig. 10:

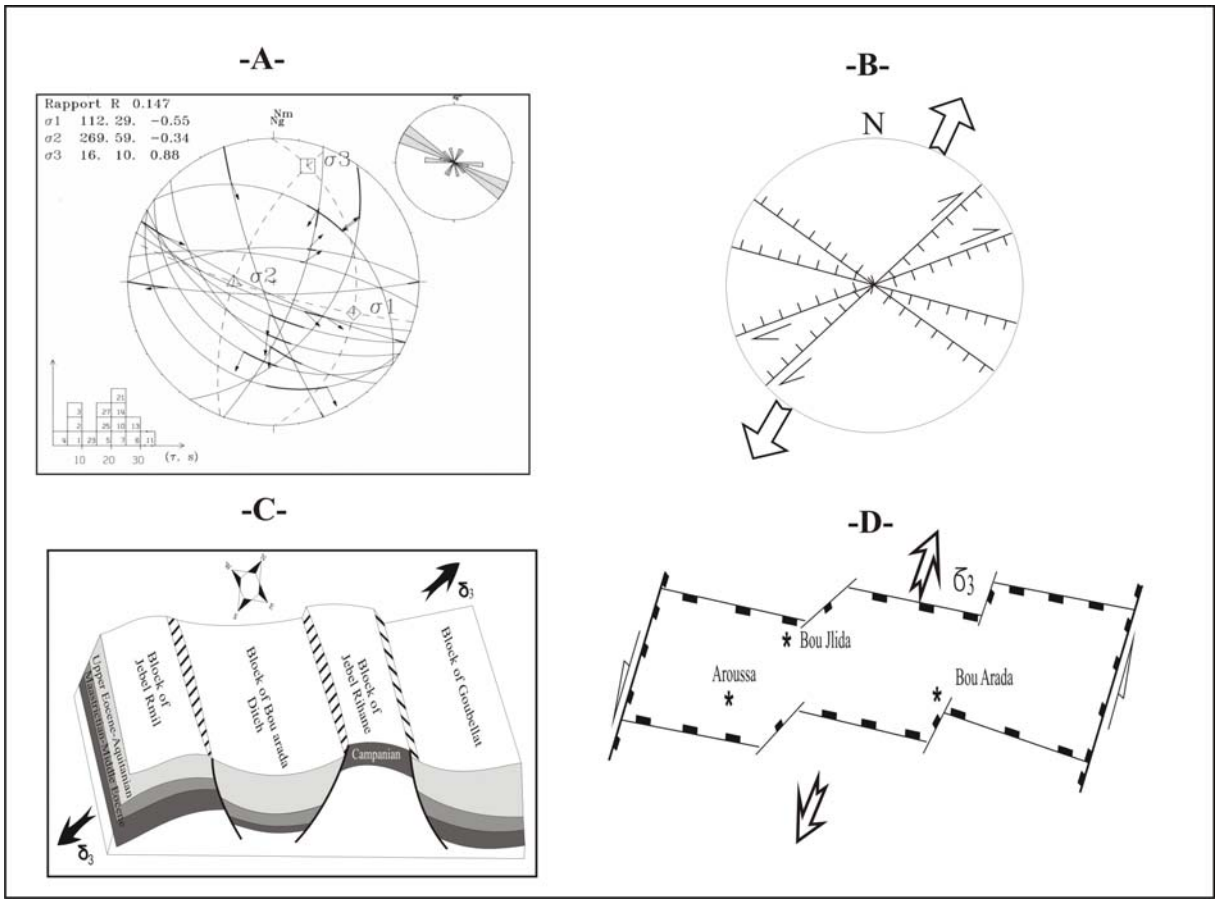
-A-
Rapport R 0.147
σ1 112. 29. −0.55
σ2 269. 59. −0.34
σ3 16. 10. 0.88
σ3
σ2
σ1
10 20 30 (τ, s)
-B-
N
-C-
Block of Jebel Rnil
Block of Bou arada Ditch
Block of Jebel Rihane
Block of Goubellat
Upper Eocene-Aquitanian
Campanian
-D-
Bou Jlida
Aroussa
Bou Arada

Fig. 11:

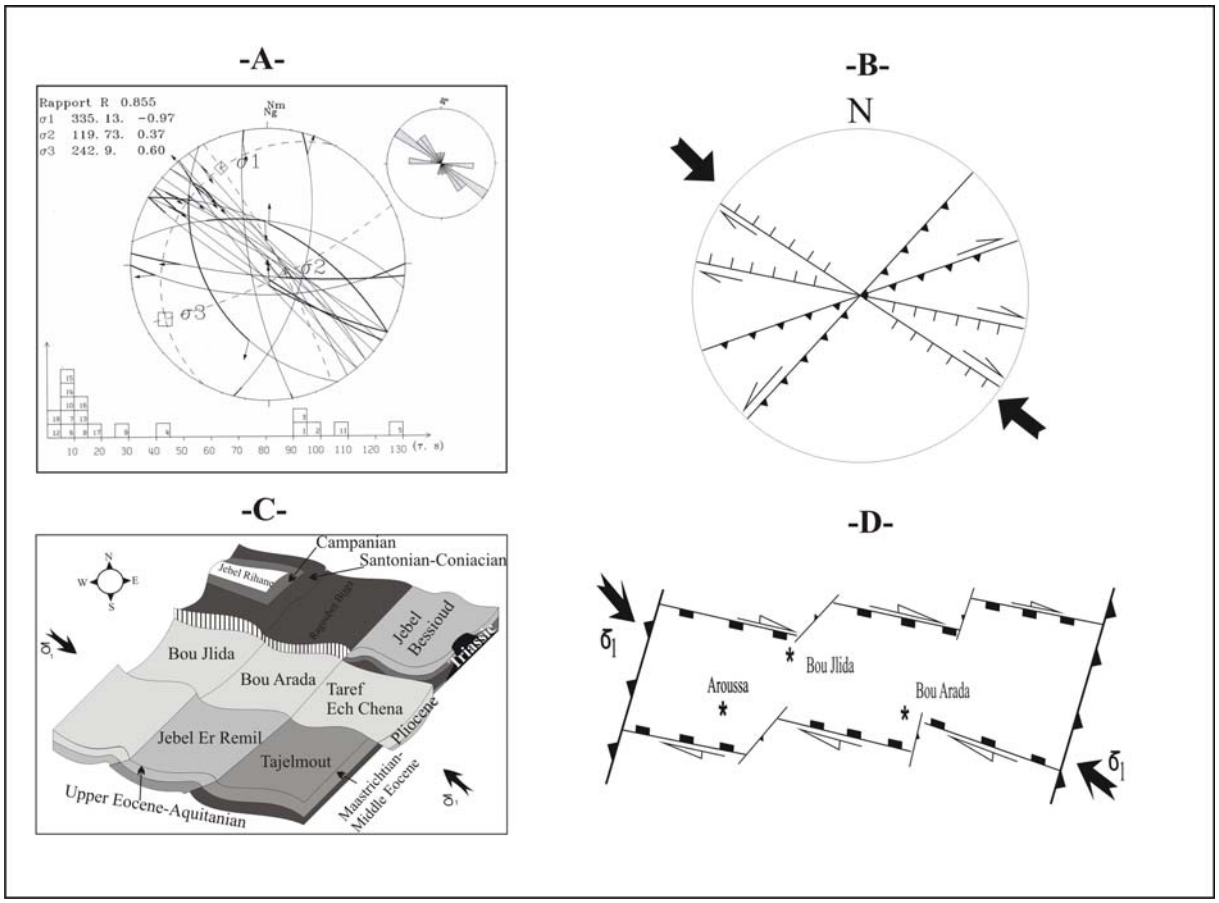
-A-
Rapport R 0.855
σ1 335. 13. −0.97
σ2 119. 73. 0.37
σ3 242. 9. 0.60
Nm
Ng
σ1
σ2
σ3
10 20 30 40 50 60 70 80 90 100 110 120 130 (τ. s)
-B-
N
-C-
N
W
E
S
Campanian
Santonian-Coniacian
Jebel Rihane
Jebel Bessioud
Bou Jlida
Bou Arada
Taref
Ech Chena
Jebel Er Remil
Tajelmout
Pliocene
Upper Eocene-Aquitanian
Maastrichtian-
Middle Eocene
-D-
σ1
Aroussa
Bou Jlida
Bou Arada
σ1

Fig. 12:

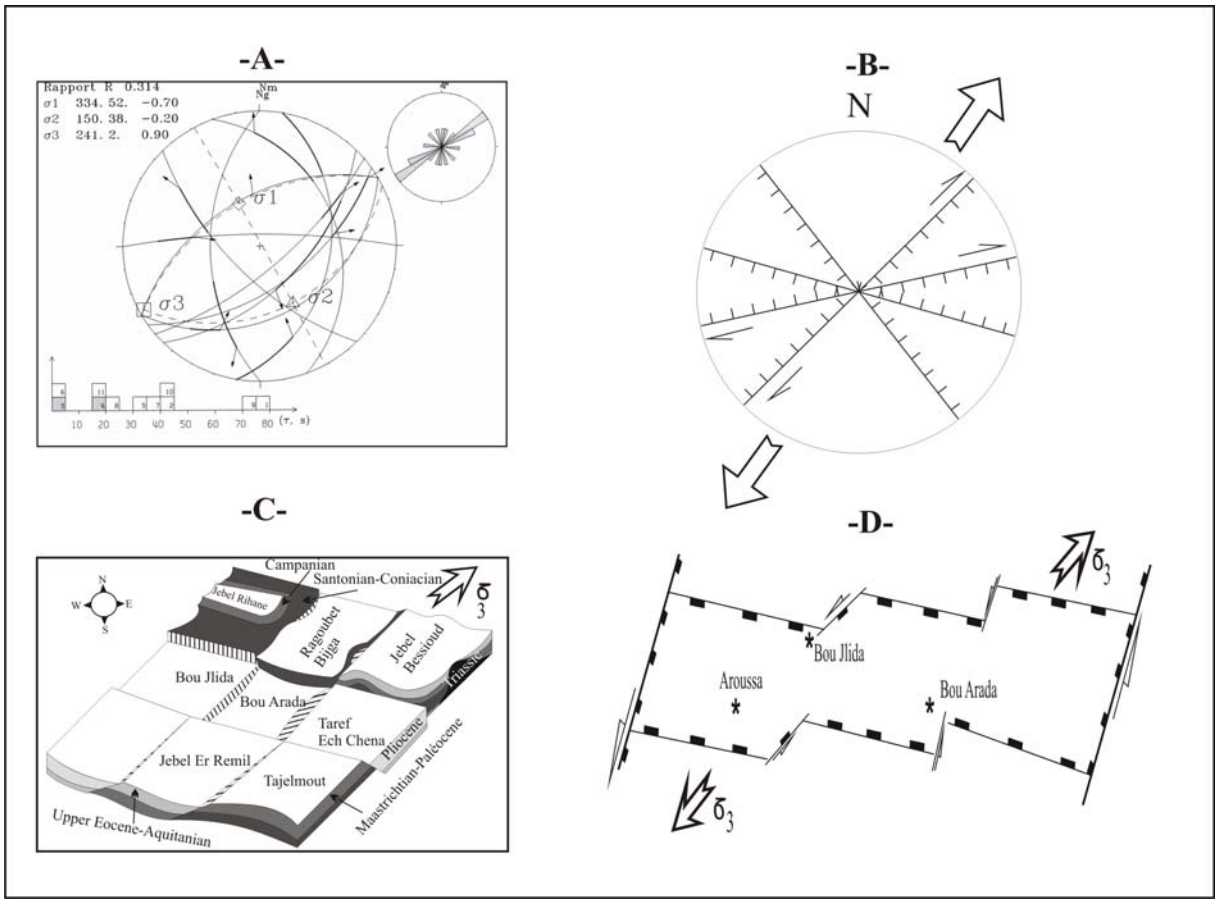
-A-
Rapport R 0.314
σ1 334. 52. −0.70
σ2 150. 38. −0.20
σ3 241. 2. 0.90
Nm
Ng
σ1
σ3
σ2
10 20 30 40 50 60 70 80 (τ, s)
-B-
N
-C-
N
W
E
S
Campanian
Santonian-Coniacian
σ3
Jebel Rihane
Ragoubet Bliga
Jebel Bessioud
Triassic
Bou Jlida
Bou Arada
Taref
Ech Chena
Pliocene
Jebel Er Remil
Tajelmout
Maastrichtian-Paleocene
Upper Eocene-Aquitanian
-D-
σ3
Bou Jlida
Aroussa
Bou Arada
σ3

Fig. 13:

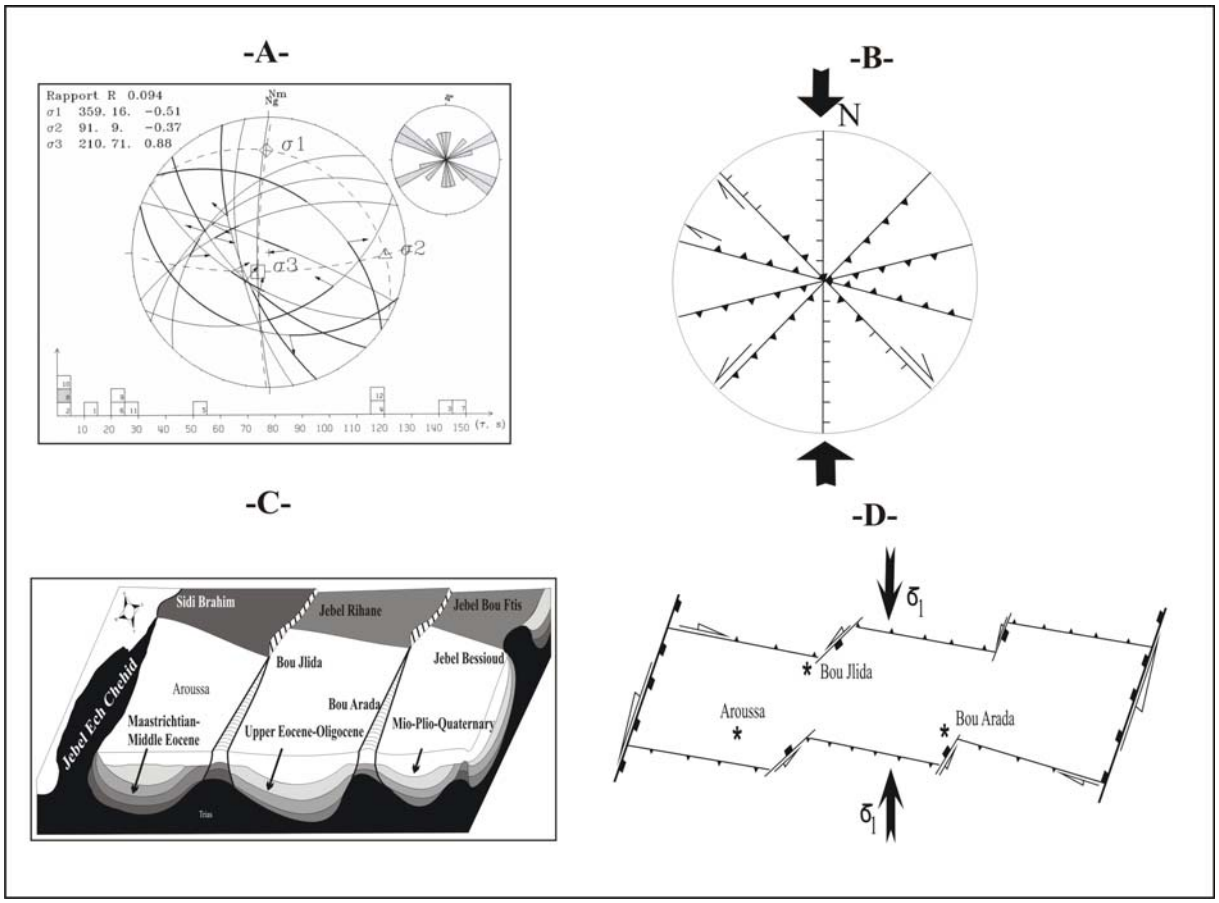
-A-
Rapport R 0.094
σ1 359. 16. −0.51
σ2 91. 9. −0.37
σ3 210. 71. 0.88
σ1
σ2
σ3
-B-
N
-C-
Sidi Brahim
Jebel Rihane
Jebel Bou Ftis
Jebel Bessioud
Bou Jlida
Aroussa
Bou Arada
Jebel Eeh Chehid
Maastrichtian-Middle Eocene
Upper Eocene-Oligocene
Mio-Plio-Quaternary
-D-
σ1
Bou Jlida
Aroussa
Bou Arada
σ1

Fig. 14:

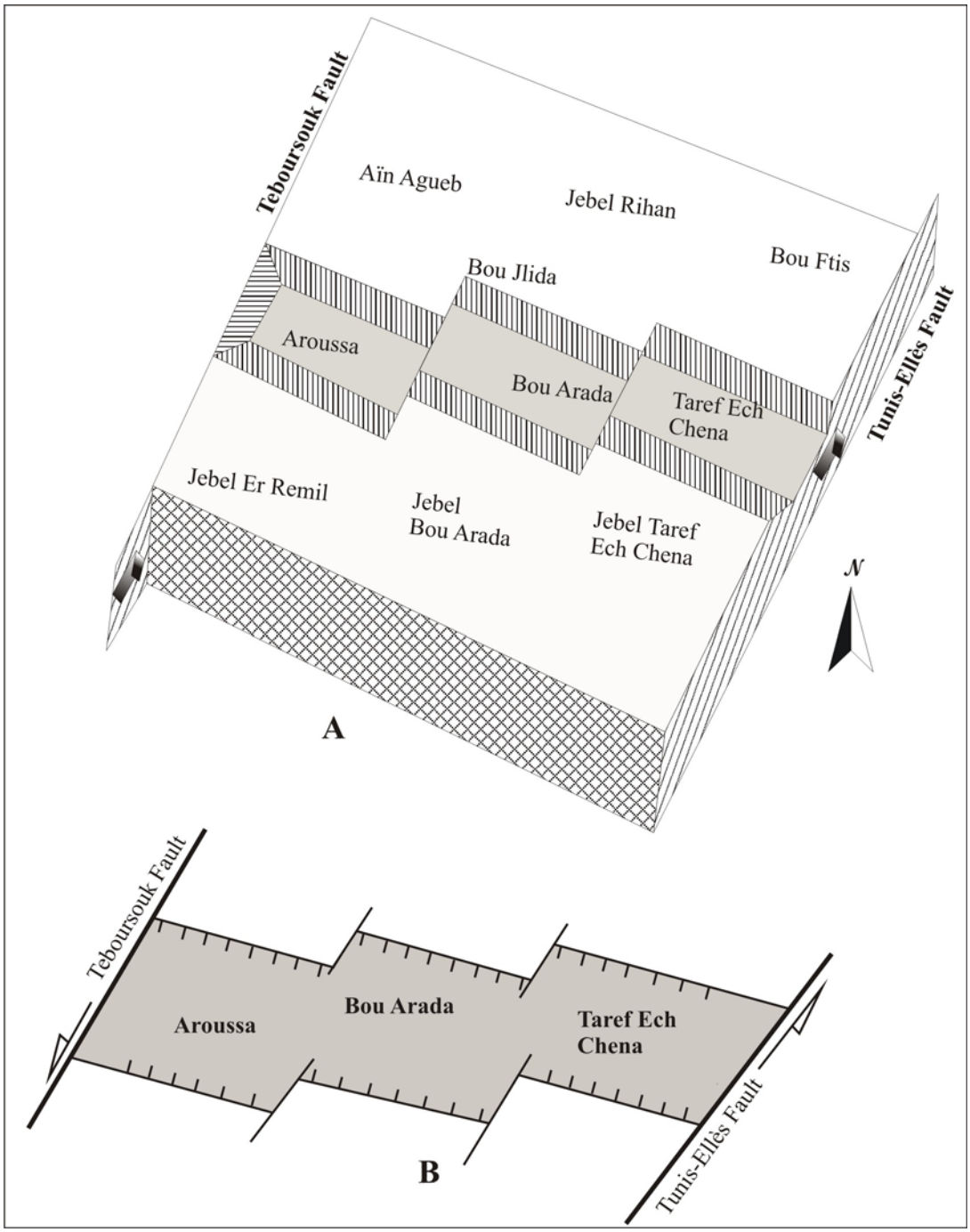
Teboursouk Fault
Aïn Agueb
Jebel Rihan
Bou Ftis
Bou Jlida
Aroussa
Bou Arada
Taref Ech Chena
Tunis-Ellès Fault
Jebel Er Remil
Jebel Bou Arada
Jebel Taref Ech Chena
N
A
Teboursouk Fault
Aroussa
Bou Arada
Taref Ech Chena
Tunis-Ellès Fault
B

Fig. 15:

882 Table 1:

Chronostratigraphy	**Formation**	**N**	**σ1**	**σ2**	**σ3**	**Φ**	**R**
Quaternary		12	359.16/ -0.51	91.9/ -0.37	210.71/ 0.88	0.094	**C**
Late Mio-Pliocene		11	334.52/ -0.70	150.38/ -0.20	241.20/ 0.9	0.314	**SS**
Middle Miocene	Beglia	18	335.13/ -0.97	119.73/ 0.37	242.9/ 0.60	0.855	**C** to **TP**
Oligocene-Aquitanian	Fortuna	15	112.29/ -0.55	269.50/ -0.34	16.10/ 0.88	0.147	**E** To **TT**
Late Eocene	Souar						
Lower Eocene	Bou Dabbous	12	319.9/ -0.95	220.44/ 0.23	58.45/ 0.77	0.696	**C** To **TP**
Paleocene	Al Haria						
Maastrichtian	Top Abiod						
Campanian	Base to Middle Abiod	05	95.63/ -0.95	202.8/ 0.35	296.26/ 0.61	0.834	**E** to **TT**